NASA CONTRACTOR REPORT

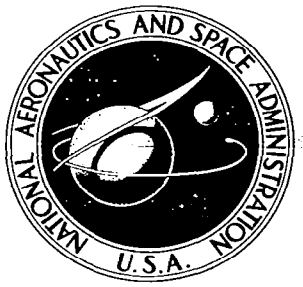

ANALYTIC AND COMPUTER STUDIES OF ELECTRON COLLECTION BY A SPHERICAL SATELLITE IN THE EARTH'S MAGNETIC FIELD

by Lee W. Parker

Prepared by
MT. AUBURN RESEARCH ASSOCIATES, INC.
Cambridge, Mass.
for Goddard Space Flight Center

NATIONAL AERONAUTICS AND SPACE ADMINISTRATION • WASHINGTON, D. C. • OCTOBER 1966

ANALYTIC AND COMPUTER STUDIES OF ELECTRON COLLECTION BY A SPHERICAL SATELLITE IN THE EARTH'S MAGNETIC FIELD

By Lee W. Parker

Prepared under Contract No. NAS 5-9228 by
MT. AUBURN RESEARCH ASSOCIATES, INC.
Cambridge, Mass.

for Goddard Space Flight Center

NATIONAL AERONAUTICS AND SPACE ADMINISTRATION

For sale by the Clearinghouse for Federal Scientific and Technical Information
Springfield, Virginia 22151 – Price $2.50

ABSTRACT

If an attempt is made to produce an artificial aurora by ejecting a beam of electrons from a satellite, the experiment will be jeopardized if the satellite potential becomes so high as to prevent the escape of the beam electrons. The buildup of potential depends on the current collection properties of the satellite. The theoretical problem considered is that of the collection of electrons by a spherical satellite in the earth's magnetic field, as a function of the satellite potential, the satellite dimensions, and the magnetic field strength. At low or intermediate positive satellite potentials, the collected current is of the order of the ambient thermal electron current collected by an area equal to twice the cross-sectional area of the satellite. At large potentials, the current rises slowly, and is proportional to V^m, where V is the potential, and m is less than unity. The value of m has been estimated theoretically in this work, by two methods. One of these methods, namely, drift approximation theory to second order, leads to an equation, involving the form of the potential distribution, from which the value of m can be found. If the potential distribution is assumed proportional to r^{-n}, where r is the radius in spherical coordinates, the value of m is found to be $2/(n+2)$. In the other method, the integrals of the exact equations of motion are analyzed to obtain rigorous bounds on the current collected. The current is found to be bounded by a value proportional to $V^{1/2}$, independent of the form of the potential distribution under reasonably general conditions. At low potentials, the current may be calculated by solving a self-consistent Poisson problem in which the charge densities depend on the form of the potential distribution. Methods for performing this calculation are discussed. The accuracy and stability of the numerical solution of the Poisson problem are shown to depend on the position of the boundary at which the potential is assumed to be zero.

TABLE OF CONTENTS

ANALYTIC AND COMPUTER STUDIES OF ELECTRON COLLECTION BY A SPHERICAL SATELLITE IN THE EARTH'S MAGNETIC FIELD

I. INTRODUCTION

The environment of a satellite moving in the ionosphere consists of a weakly ionized plasma in a magnetic field. The satellite usually has an electrostatic potential different from that of the plasma, partly due to the currents of ionospheric ions and electrons striking the satellite, and partly due to the emission from the satellite of charged particles, such as photoelectrons, secondary electrons, or artificial beams of ejected charged particles.

The problem of concern in this report is that of a satellite which emits artificially a beam of 1 ampere of relatively high-velocity electrons. The satellite will become positively charged as a result of this emission. The potential attained by the satellite is to be determined under the following conditions. The satellite, of radius 1.5 meters, is considered to be at an altitude of about 200 km, where it is assumed that the temperature is 1500°K, the magnetic field strength is 0.45 gauss, and the electron density is $7.2 \times 10^4/cm^3$. The Debye length is 1.0 cm, and the mean thermal Larmor radius is 2.7 cm. The mean ambient thermal electron current is 0.7 milliamperes per square meter. It is important to note that the emitted current is of the order of 100 times the thermal electron current passing into an area twice the cross-sectional area of the sphere.

The satellite potential is determined by the condition that there be no net current to the satellite. In the absence of emitted currents, the equilibrium potential of the satellite has that value for which the currents of electrons and positive ions passing into the surface from the ambient plasma are equal. This potential is normally negative, since the ambient electron currents are greater than the ambient ion currents, and is of the order of kT/e, where

T is the temperature of the plasma, k is the Boltzmann constant, and e is the electron charge. In the presence of photoelectron emission, secondary electron emission, or artificial electron beam emission, the equilibrium potential shifts toward positive values. If the artificial electron beam current becomes the dominant current passing out of the surface, the equilibrium potential rises to a positive value, tending to attract a compensating current of electrons from the plasma. If the equilibrium potential exceeds the beam particle kinetic energy, the ejected particles cannot escape. Thus, there is a maximum current of electrons which can be emitted, depending on the energy of the beam particles and on the current-collecting characteristics of the satellite as a function of the satellite potential (i.e., the "current characteristic"). The electron current collected increases monotonically with the satellite potential. Hence, the upper bound on the current which can be emitted is that current corresponding to the potential equivalent of the beam particle energy. In this sense, the problem of determining the limitation on current emission is identical to the problem of determining the current characteristic of an electrostatic probe in a plasma. Of special importance is the "saturation" part of the characteristic, since there the current only increases very slowly as a function of potential. This means that when the emitted current is near the saturation value, the potential tends to rise very rapidly. The object of the work reported here is to apply analytic and computer methods to determine the behavior of the saturation portion of the current characteristic of a sphere immersed in a plasma in a strong magnetic field.

The current characteristic of a satellite in the presence of the earth's magnetic field is greatly different from what it would be in the absence of the magnetic field. Since the magnetic field effect is crucial, it will now be discussed further. In the ionosphere, Larmor (or gyration) radii of electrons are on the order of centimeters while satellite dimensions are on the order of meters.

Moreover, electron collision mean free paths are on the order of kilometers. Hence, electrons move easily along the magnetic field lines, but remain "glued" to the field lines while executing very tight spiral motions around them. Although the mean free paths are very long, collisions and other stochastic processes cause a slow diffusion across the field lines. The effect of this diffusion is probably negligible, although theoretical estimates of its magnitude are difficult to make[1,2] in the absence of an adequate theory. A drift also occurs across magnetic field lines under the action of inhomogeneous electric fields, as predicted by the well known theory of the guiding-center drift.[2,3] This "electrical drift" arises from a second-order term in the drift approximation expansion and is normally small. The rate of this drift increases as the electric field strength increases. However, unless the electric field is enormous, the electrons which can be collected are limited to those which move along the magnetic field lines from "infinity" (kilometers away) to the satellite. That is, if the magnetic field within a kilometer or so is considered to be uniform, the maximum or "saturation" current collected by the satellite is ordinarily the thermal electron current (0.7 ma/m^2 in the present case) which is collected by an area approximately equal to twice the cross-sectional area (14 m^2 in the present case) of the satellite normal to the field lines. (The collection area is slightly larger than this due to the finite Larmor radius.) The geometric aspect of the problem is shown in Fig. 1, in which the satellite, assumed without loss of generality to be a sphere (of radius 1.5 m in the present case), is inscribed in an infinite cylinder of the same cross-sectional area, oriented parallel to the magnetic field. The thermal electron current entering the end-caps at infinity, which in the ionosphere is on the order of 10 milliamperes, is collected by the sphere when its potential is positive and of order kT/e or greater. The current diffusing through the walls of the cylinder may be expected on the basis of

classical collision theory to be less than the thermal value by the ratio of the Larmor radius to the sphere radius.[1] Experimentally, the collected current is indeed small compared with the thermal value, although it is somewhat larger than the classical value.[1] Therefore, it is reasonable to assume here that diffusion by stochastic processes is negligible, and we will investigate only the electrical effects.

As the potential of the satellite increases, the second-order electrical drift due to the inhomogeneous electric field increases, and the current collected increases, though very slowly. The current characteristic of the satellite essentially exhibits a saturation, i.e., the current-voltage curve is very nearly flat. It is shown in Secs. II, III, and IV of this report that a large enhancement of current over the thermal value requires enormous satellite potentials. For example, a satellite 1.5 meters in radius, in a magnetic field of strength 0.45 gauss, must have a potential of at least 10^6 volts (based on non-relativistic dynamics in Sec. III) in order to collect 100 times the thermal current, i.e., 1 ampere. This result is at variance with the implications of a paper by Beard and Johnson[4] on the current collection by a spherical satellite. According to their formulae, the satellite need only have about 10^4 volts in order to collect 1 ampere of current. This is based on the assumption of a Coulomb electric field in the vicinity of the satellite, which may be justified on the grounds that the satellite potentials of interest are large (compared with kT/e) and that the extent of the electric field, i.e., the sheath thickness, is correspondingly very great. However, Beard and Johnson do not take angular momentum effects into account, and, more important, assume without justification that the magnetic field can be neglected for the satellite potentials of interest, since they believe that the magnetic field effects will be "dominated" by the electric field effects. The latter assumption is invalid, according to the results of the present

investigation, unless the potentials are orders of magnitude greater than the potentials considered by Beard and Johnson.

In Secs. II, III, and IV, comprising Part I of this report, the potential is assumed to be a Coulomb potential in the vicinity of a spherical satellite, with an arbitrary potential on the sphere. The magnetic field is assumed to have a value of 0.45 gauss, a typical value in the ionosphere, and the sphere is assumed to have a radius of 1.5 meters.

In Sec. II, the current collection based on the theory of the drift approximation is calculated as a function of sphere potential V, and is shown to be proportional, for large potentials, to $V^{2/3}$ for a Coulomb potential, and to $V^{2/(n+2)}$ for a power-law potential falling off as r^{-n}. The power-law potential is invoked to represent the effect of shielding, i.e., a rapid drop-off in potential. According to the drift theory, a 100-fold increase in current collection over the thermal value requires a sphere potential of at least 2×10^5 volts.

In Sec. III, the dynamical equations (non-relativistic) of an electron in a spherically symmetric potential are analyzed in order to obtain rigorous bounds on current collection. A 100-fold increase in current collection over the thermal value is found to require a sphere potential of at least 10^6 volts. The discrepancy between this value and the lower one given by the drift approximation theory may be attributed to the neglect, in the drift theory, of the conservation of canonical angular momentum. Thus, centrifugal forces, which tend to keep the electron away from the axis of the system, are neglected in the drift theory. It is shown that current collection, for large potentials, cannot increase more rapidly than $V^{1/2}$. As a result of the analysis, it is possible to define surfaces in cylindrical space, i.e., "bottles," within which the trajectories are confined.

In Sec. IV a number of exact trajectory calculations are presented, for an electron moving from infinity toward the vicinity of a sphere of radius 1.5 meters, in a magnetic field of 0.45 gauss. A Coulomb electric field is assumed, and in all trajectory calculations the sphere is assumed to have a potential of 1.294×10^7 volts, corresponding to 10^8kT. This potential was inadvertently chosen to be higher than the potentials of interest. It would give an enhancement factor in current collection of 1600 on the basis of the drift approximation and 360 on the basis of the dynamical limitations of Sec. III. Nevertheless, these calculations are of interest in demonstrating how the analysis of Sec. III may be applied to problems of this type of quasi-confinement of electrons. Some of the trajectories are extremely complicated, and electrons having small positive total energy may spend a great deal of time in the vicinity of the sphere. For all of the trajectories calculated, the initial condition corresponds to electrons incident at infinity, moving initially along various magnetic field lines. Due to the rotational symmetry, the drift of the electrons causes them to move on cylindrical surfaces, or "magnetic shells", defined by the radial distance of the initial field lines from the axis. Figure 1 illustrates magnetic shells which may or may not intersect the sphere. If the radius of the magnetic shell is sufficiently small, the electron will move on it until it reaches the vicinity of the sphere, at which point it "breaks away" and moves in toward the sphere. If it does not strike the sphere on the first pass, it may bounce a great deal within the bottle before either striking the sphere or passing out again to infinity, on the original magnetic shell. The space within the confining bottle is, in some cases, well covered by the path of the electron.

The material in Secs. II, III, and IV, discussed above, comprises Part I of this report, which is concerned with the current collection by a spherical satellite having large potentials. That

is, Part I is concerned with the "saturation" behavior of the current characteristic.

For intermediate and small potentials, i.e., for potentials not very large compared with kT/e, the shape of the current characteristic is more difficult to ascertain. This regime applies to problems concerning the equilibrium potential of a satellite or, equivalently, the characteristics of an electrostatic plasma probe in a magnetic field. Even in the absence of a magnetic field, theoretical progress on the probe problem has been very slow since the work of Langmuir and his associates.[5] This is due, to some extent, to numerical difficulties, to be described later.[6-9] In the presence of a magnetic field, there has been almost no progress at all.[10] The material in Secs. V, VI, and VII is concerned with the latter problem and comprises Part II of this report. A computational procedure is being developed for the purpose of calculating the sheath structure, i.e., the potential distribution in the vicinity of the sphere in the presence of a magnetic field. This program has not yet been completed. However, some progress has been made in the understanding of the computational nature of the problem. This should be useful in future work on the probe problem.

A general computational approach for determining the potential and charge density distributions in a self-consistent manner is described in Sec. V. This approach employs a discretization of space in the form of a grid, and the charge densities and potentials are evaluated at the points of the grid. The problem is to be solved for a number of fixed sphere potentials, and the net current collected is to be calculated for each sphere potential, thus yielding the current characteristic in tabular form.

In order to test the program, calculations were performed on a spherically symmetric problem with the magnetic field turned

off. These calculations are described in Sec. VI. They were begun with the double purpose of checking on the operation of the program for relatively short runs, and to afford possible comparison with earlier calculations performed on spherical probes.[6,7] It was soon learned, however, that the treatment of the boundary condition requiring the potential to vanish at infinity introduces a fundamental numerical difficulty. Because of the importance of this difficulty, it will now be discussed further. Since the calculations must be performed on a grid of finite dimensions, the potential is usually set to zero on the outer boundary points of the grid. The position of the outer boundary of the grid must be sufficiently far from the sphere that its exact position does not affect the solution. On the other hand, as the boundary is moved to greater distances, the difficulty of obtaining a solution increases in that the solution becomes unstable. The instability manifests itself in the iterative procedure for developing the self-consistent solution, in that successive iterates tend to diverge and become meaningless. Thus, the accuracy of a numerical solution is difficult to assess. Examples of this behavior are given in Sec. VI. It was found that the procedure adopted in Sec. VI became unstable as the boundary was moved out, and that the instability was associated with large radial distances where the potentials were small compared with kT. At these great distances, where the net charge density is small compared with n_o, large contributions occur, and therefore care must be used in summing these contributions.

Relatively little attention, that is, in the form of published reports or papers on probe and satellite space charge calculations, appears to have been given to the instability problem. An exceptional paper in this regard is that of Bernstein and Rabinowitz[6], who caution that care must be used when computing the potential at large distances from a spherical or cylindrical probe. Their procedure was applied to a monoenergetic distribution of

particles, but it does not appear to be applicable to more general problems such as the subject of this report. A report of interest is that of Hall[8], who developed an integral formulation for the spherical and cylindrical probe, where the form of the charge density function, rather than its value, must be guessed at in an iterative scheme. This formulation depends on the assertion[6] that the potential falls off at large distances like the inverse square of the radius, for the spherical probe. Hall and Freis[9] applied this formulation to the cylinder, but it has not been applied to the sphere. It cannot be applied to the present problem.

Among the most interesting numerical solutions which have been published on the distribution of potential around moving satellites are those of Davis and Harris[11] and of Hohl and Wood[12]. These workers apparently did not explore the effect of the boundary position, but rather chose it to be sufficiently near the sphere to render their iteration procedures convergent. Since the effect of moving the boundary was not ascertained, the accuracy of these calculations cannot be assessed.

Other procedures have been attempted in the interest of developing greater stability in the calculations. Based on the inverse-square-law assertion for the spherical probe problem[6], Laframboise[7] adopted the condition that at the finite boundary of his grid, the potential, instead of vanishing, be proportional to r^{-2}. Under these circumstances, he found that the solution was relatively insensitive to the position of the boundary. However, he found it necessary to use care in the iteration process, and adopted a scheme in which successive density iterates were coupled. The present author[13] encountered instabilities in the process of computing the potential in the vicinity of a planar ion and electron trap mounted in the skin of a satellite. The potential was assumed to be given by a power law at the boundary of the grid, but the solution

was unstable when the boundary was moved out beyond a certain point. The coupling of successive density iterates allowed the boundary to be moved out slightly further, but this method cannot be regarded as generally satisfactory.

Thus, a great deal of work remains to be done on this problem.

In Sec. VII, simplified semi-analytic expressions are derived for the electron density in the presence of a strong magnetic field. The motivation for this is that trajectory calculations take up a great deal of computer time when the Larmor radius is small compared with the sphere radius, and, in employing the general method described in Sec. V for computing particle densities, a large number of trajectories must be calculated. It should prove fruitful, in the theory of a probe in a strong magnetic field, to make use of the drift approximation as in Sec. VII, to estimate the density of electrons, i.e., the attracted particles. This has not been done previously, to the author's knowledge. According to the drift approximation, electrons (i.e., their guiding-centers) will move on the surfaces of cylindrical shells concentric with the axis of the system. Figure 1 illustrates these surfaces. If the contribution to the density due to the transverse ExB motions is considered negligible compared with the contribution due to longitudinal motions, the density may be calculated as if the electrons moved along rigid straight lines, parallel to the magnetic field direction.

This model has not been developed into a computer code, but may be done so relatively easily.

PART I

ELECTRON COLLECTION AT LARGE POTENTIALS

Sec. II Current Collection According to the Drift Approximation

Sec. III Rigorous Dynamical Bounds on Current Collection

Sec. IV Exact Trajectory Calculations

II. CURRENT COLLECTION ACCORDING TO THE DRIFT APPROXIMATION

The equation which describes the drift of electrons, in a strong magnetic field, toward the axis of the system under a rotationally symmetric electric field, may be derived on the basis of the theory of the drift approximation. This theory describes the motion of the guiding-center of an electron in non-homogeneous electric and magnetic fields. A non-rigorous method of deriving the appropriate equation is the following one. It is based on the expansion of the velocity in the equation of motion in a power series with respect to m/e, i.e., the ratio of electron mass to electron charge[2]. We will perform this expansion with the understanding that the magnetic field is uniform, while the electric field is rotationally symmetric.

The equations of motion of an electron in an electric field and a constant magnetic field may be resolved in components perpendicular and parallel to the magnetic field, as follows:

$$\dot{\vec{V}}_\perp = -\frac{e}{m}\vec{E}_\perp - \frac{eB}{mc}\left(\vec{V}_\perp \times \hat{k}\right) \qquad (e>0) \tag{1}$$

$$\dot{\vec{V}}_\parallel = -\frac{e}{m}\vec{E}_\parallel \tag{2}$$

where $\vec{V}$ is the velocity, $\vec{E}$ is the electric field, B is the magnitude of the magnetic field, $\hat{k}$ is a unit vector in the direction of the magnetic field, and the dot denotes the derivative with respect to time. The subscripts $\perp$ and $\parallel$ denote components perpendicular and parallel, respectively, to the direction of $\hat{k}$. Equation (2) could have been written as a scalar equation, but $\vec{V}_\perp$ and $\vec{E}_\perp$ in Eq. (1) must be described by two components in the plane perpendicular to $\hat{k}$.

Let $\vec{V}_\perp$ be given by a formal power series in the quantity ω^{-1}, where $\omega \equiv eB/mc$, as follows:

$$\vec{V}_\perp = \sum_{n=0}^{\infty} \omega^{-n} \vec{V}_n \tag{3}$$

Substituting this expansion into Eq. (1), we have

$$\sum_{n=0}^{\infty} \omega^{-n} \dot{\vec{V}}_n = -\omega \frac{c}{B} \vec{E}_\perp - \sum_{n=0}^{\infty} \omega^{-n+1} \left(\vec{V}_n \times \hat{k} \right) \tag{4}$$

Equating the coefficients of ω, 1, ω^{-1}, ω^{-2}, etc. to zero, we obtain the set of coupled equations:

$$\hat{k} \times \vec{V}_0 = \frac{c}{B} \vec{E}_\perp \tag{5}$$

$$\hat{k} \times \vec{V}_1 = \dot{\vec{V}}_0 \tag{6}$$

$$\hat{k} \times \vec{V}_2 = \dot{\vec{V}}_1 \tag{7}$$

etc.

The solution of this set of equations is:

$$\vec{V}_0 = \frac{c}{B} \vec{E}_\perp \times \hat{k} = -\hat{k} \times \frac{c\vec{E}_\perp}{B} \tag{8}$$

$$\vec{V}_1 = -\hat{k} \times \vec{V}_0 = \hat{k} \times \hat{k} \times \frac{c\dot{\vec{E}}_\perp}{B} \tag{9}$$

$$\vec{V}_2 = -\hat{k} \times \vec{V}_1 = -\hat{k} \times \hat{k} \times \hat{k} \times \frac{c\ddot{\vec{E}}_\perp}{B}$$

$$= \hat{k} \times \frac{c\ddot{\vec{E}}_\perp}{B} \tag{10}$$

etc.

as may be verified by substitution, where it is understood that $\vec{V}_n \cdot \hat{k}$ vanishes for all vectors $\vec{V}_n$.

Thus, the drift approximation equation for the transverse motion of the guiding center may be written

$$\vec{V}_\perp = \frac{c}{B}\left(-\hat{k} \times \vec{E}_\perp + \frac{1}{\omega}\hat{k} \times \hat{k} \times \dot{\vec{E}}_\perp + \frac{1}{\omega^2}\hat{k} \times \ddot{\vec{E}}_\perp + \cdots\right) \tag{11}$$

This equation is consistent with one derived for the guiding center motion by Northrop (Reference 3, p. 8). Northrop's equation, which applies to varying magnetic and electric fields, reduces to the first two terms of Eq. (11) for a constant magnetic field. The third term in Eq. (11) is not given by Northrop's equation. It is of higher order than is required here and will be ignored within the present approximation. The first and second terms in Eq. (11) will be denoted the "first-order" and "second-order" drift terms, respectively, in keeping with the usage of these terms in the literature.

Since the electric field considered here is constant in time, the time-derivative of the second-order term involves the velocity of the electron, as follows:

$$\dot{\vec{E}}_\perp = \vec{V} \cdot \nabla \vec{E}_\perp \tag{12}$$

The electrostatic potential considered here is rotationally symmetric. Hence, a cylindrical coordinate system is conveniently employed, in which r, θ, and z denote the radial, azimuthal, and axial coordinates, respectively. The unit vectors along these directions will be denoted by $\hat{r}$, $\hat{\theta}$, and $\hat{k}$, respectively, where $\hat{k}$ is in the direction of the magnetic field. Thus, $\vec{E}_\perp$ is given by

$$\vec{E}_\perp = E_r \hat{r} \tag{13}$$

Using the first two terms of Eq. (11), the drift velocity, to first order in ω^{-1}, becomes:

$$\vec{V}_\perp = -\frac{c}{B} E_r \hat{\theta} + \frac{c}{\omega B}\left[\frac{c}{B}\frac{E_r^2}{r}\hat{\theta} - V_z \frac{\partial E_r}{\partial z}\hat{r}\right]$$

$$+ \bigcirc(\omega^{-2}) \tag{14}$$

The signs of the second-order terms in Eq. (14), i.e., the terms in the brackets, will be reversed for a positively charged particle.

The terms in Eq. (14) have been discussed by Bertotti[2]. The first term involving $\hat{\theta}$ represents the familiar ExB azimuthal drift. The second term involving $\hat{\theta}$ represents an azimuthal second-order diamagnetic drift current. The term involving $\hat{r}$ represents the radial component of the second-order drift which is of interest in this report. Ignoring for the moment the terms involving $\hat{\theta}$, an electron (guiding center) moving along a line parallel to the z-axis would experience a radially inward, or a radially outward, second-order drift, depending on whether it sees an (algebraic) decrease or increase in E_r as it moves along, respectively. If the source of the electric field were a positive point charge (i.e., an attractive Coulomb field), $-E_r$ would be always negative and would decrease if the electron were to move along the line in the direction of decreasing separation from the positive charge. That is, if the electron moves so as to be nearer to the positive charge, its guiding center drifts radially <u>inward</u> as well. The conclusion is the same when the transverse ExB drift is included, since to lowest order the electron guiding center describes a helix on the surface of a cylinder, and it is the axial component of this motion which gives rise to the inward drift. In terms of the electrostatic potential energy Φ, the radially inward drift velocity of the guiding center, from Eq. (14), may be written

$$V_r = - V_z \frac{1}{m\omega^2} \frac{\partial^2 \Phi}{\partial r \partial z} \tag{15}$$

A. THE INWARD DRIFT

It will be of interest to compute in some detail the radially inward drifts of an electron which finds itself in combined magnetic and electric fields. The magnetic field will be taken to be uniform over the dimensions of interest in the problem, and to have a strength of 0.45 gauss, which is typical of the earth's magnetic field in the

ionosphere. The electric field will be taken to be the spherically symmetric Coulomb field which would exist in the vicinity of a spherical satellite of radius 1.5 m, charged to an arbitrary positive potential, in the absence of significant space charge shielding by the electrons in the ambient ionosphere. It is desired to know the area at infinity from which electrons can be collected by the sphere, as a function of the sphere radius, sphere electrostatic potential, and the strength of the magnetic field. In the absence of inward drift, or if the sphere is uncharged, the collection area at infinity is exactly equal to that of the cross-section of the sphere (neglecting the slight enhancement due to the finite Larmor radius).

The radius of the collection area at infinity may be obtained from the solution of a first-order time-independent differential equation derived from Eq. (15), namely

$$\frac{dr}{dz} = -\frac{1}{m\omega^2}\frac{\partial^2 \bar{\Phi}}{\partial r \partial z} \tag{16}$$

where $\bar{\Phi}(r,z)$ is a known axially symmetric function representing the electrostatic potential energy of an electron in the vicinity of the sphere. Equation (16) is to be solved subject to the condition that r be equal to the sphere radius when z lies on the equatorial plane of the sphere. Let the center of the sphere be at z = 0, so that the equatorial plane corresponds to z = 0. Then the solutions have the form depicted in Fig. 2. The slope dr/dz = 0 at z = 0 because of the symmetry of $\bar{\Phi}$, and dr/dz = 0 at $z = \infty$ because $\bar{\Phi}$ and its derivatives vanish at infinity. Assuming the right-hand-side of Eq. (16) does not change sign, the function r increases monotonically from the value of the sphere radius at z = 0 to a limiting value, greater than the sphere radius, at $z = \infty$. This limiting value is taken to define the radius of the collection area at infinity.

Let Φ be given by the attractive Coulomb form:

$$\Phi = -\frac{\Phi_o a}{(r^2+z^2)^{1/2}} \qquad \Phi_o > 0 \tag{17}$$

where Φ_o is the magnitude of the potential energy of an electron at the surface of the sphere. Denoting by a the sphere radius, and letting r_1 and z_1 denote r/a and z/a, respectively, Eq. (16) becomes

$$\frac{dr_1}{dz_1} = \alpha \frac{r_1 z_1}{(r_1^2 + z_1^2)^{5/2}} \tag{18}$$

where

$$\alpha \equiv \frac{3\Phi_o}{m\omega^2 a^2} = 1.71 \times 10^{-3} \frac{V\,(\text{volts})}{[a\,(\text{meters})]^2[B\,(\text{gauss})]^2} \tag{19}$$

where V (volts) is the potential on the sphere in volts, a (meters) is the sphere radius in meters, and B (gauss) is the strength of the magnetic field in gauss.

Assuming a sphere radius of 1.5 meters and B = 0.45 gauss, α becomes

$$\alpha = 3.75 \times 10^{-3}\, V\,(\text{volts}) \tag{20}$$

The solution of Eq. (18) is subject to the condition that $r_1(z_1 = 0) = 1$.

Solutions of Eq. (18) have been obtained numerically for a number of values of sphere potential. The results are given in Figs. 2 and 3, and in Table I. It may be inferred from Fig. 3 or Table I that a 100-fold increase in current-collecting ability ($(r_\infty/a)^2 = 100$) is not

achieved until the sphere potential is about 2×10^5 volts. Also apparent from Fig. 3 or Table I is the fact that r_∞ becomes proportional to $V^{1/3}$ (i.e. to $\propto^{1/3}$) as V becomes very large (>1000 volts). The relative insensitivity of r_∞ to V illustrates the difficulty of causing electrons to drift across the magnetic field lines through the agency of large electric fields alone.

The solutions discussed above are based on the assumption of an unshielded electrostatic field, i.e., a Coulomb potential. Some insight regarding the effect of a shielded field may be afforded by consideration of spherically symmetric potentials which fall off more rapidly than the Coulomb potential. The fact that the actual shielded field is not spherically symmetric is probably not as important as the fact that the potential falls off rapidly. As a model potential, one may adopt a finite sheath thickness model or a power-law model, for example. These two models have been shown by Parker[14] to be essentially equivalent characterizations of the form of the potential, with regard to the current-collecting characteristics of spherical probes. The power-law model will be adopted here. If the potential falls off as R^{-n}, where R is the spherical radius, we have, instead of Eq. (17),

$$\Phi = -\frac{\Phi_0 a^n}{(r^2+z^2)^{n/2}} \qquad \Phi_0 > 0 \tag{21}$$

and instead of Eqs. (18) and (19),

$$\frac{dr_1}{dz_1} = \alpha \frac{r_1 z_1}{(r_1^2+z_1^2)^{\frac{n}{2}+2}} \tag{22}$$

where

$$\alpha \equiv \frac{n(n+2)\Phi_0}{m\omega^2 a^2} \tag{23}$$

If we transform to the new variables $s = r_1/\alpha^{\frac{1}{n+2}}$ and $t = z_1/\alpha^{\frac{1}{n+2}}$ then Eq. (22) becomes

$$\frac{ds}{dt} = \frac{st}{(s^2+t^2)^{\frac{n}{2}+2}} \tag{24}$$

The solution satisfies the condition $s(t = 0) = 1/\alpha^{\frac{1}{n+2}}$. In the asymptotic regime, where α becomes large, i.e., where the potential V on the sphere becomes large, $s(t = 0)$ approaches zero. Hence, since Eq. (24) is free of parameters, and since $s \cong 0$ for $t = 0$ in the asymptotic regime, the value of $s_\infty \equiv \lim_{t\to\infty} s$ approaches a constant of the order of unity. That is, asymptotically, solutions of Eq. (24) exhibit a similarity behavior. Thus, in the asymptotic limit, the solution at infinity of Eq. (22) has the form

$$r_{1\infty} = \frac{r_\infty}{d} \sim \alpha^{\frac{1}{n+2}}\, s_\infty \sim \alpha^{\frac{1}{n+2}} \tag{25}$$

where s_∞ is of the order of unity and $\alpha^{\frac{1}{n+2}}$ is large compared with unity. The asymptotic behavior described here is borne out by the exact solutions of Eq. (18) for the Coulomb case, where $n = 1$. Table I shows that when $\alpha^{1/3}$ is larger than unity, r_∞ is indeed proportional to $\alpha^{1/3}$. Moreover, r_∞/a is approximately equal in magnitude to $\alpha^{1/3}$. Thus, the case of n larger than unity, which represents the effect of shielding, results in an even slower increase of the collection radius with sphere potential than the Coulomb case with $n = 1$.

The drift approximation must break down for sufficiently large electric fields, i.e., when the electric field E is comparable with or larger than the magnetic field B. This would occur, for the case of interest here, when E is of the order of

0.45 statvolts per centimeter, or 0.15 volts per meter. If R is the spherically radial distance from the center of the sphere, which has radius a and electrostatic charge Q, then E > B if:

$$R^2 < R_b^2 \equiv \frac{\Phi_o a}{eB} \tag{26}$$

where Φ_o is defined as the potential energy of an electron at the surface of the sphere. Since Φ/e (statvolts) = V (volts)/300, we have:

$$\frac{R_b^2}{a^2} = \frac{V(\text{volts})}{3 \times 10^4 \times a(\text{meters}) \times B(\text{gauss})} \tag{27}$$

or,

$$\frac{R_b}{a} = 0.7 \times 10^{-2} \sqrt{V(\text{volts})} \tag{28}$$

Thus, the breakdown occurs at the sphere surface when V is 2×10^4 volts, and at 3 sphere radii when V is 2×10^5 volts. However, according to Table I and Fig. 3 based on the drift approximation, the collection radius at infinity is 10 sphere radii (100-fold enhancement in current collection) for a sphere potential of 2×10^5 volts. Thus, the collection radius at infinity is, for this potential, somewhat greater than the "breakdown" distance, and the drift approximation should be valid until the electron has undergone an appreciable inward drift.

The argument concerning the validity of the drift approximation (Eq. (18)), with regard to breakdown at high electric field strengths, can be generalized in the following way. It may be inferred from Eqs. (25) and (26) that the drift approximation will

not break down in a Coulomb electric field, provided that

$$r_\infty \sim a\alpha^{1/3} > R_b \tag{29}$$

Using the definition for α of Eq. (19), the inequality of Eq. (29) may be rearranged in the form:

$$\frac{eB\Phi_0 a}{9m^2c^4} < 1 \tag{30}$$

or,

$$\frac{\Phi_0}{mc^2} < \frac{9c}{\omega a} \tag{31}$$

Thus, for the case at hand, where a = 150 cm and ω = eB/mc = 1.755×10^7 sec^{-1}, the right-hand-side of Eq. (31) is 228. Since $mc^2 = 5\times10^5$ electron-volts, the drift approximation results given in Table I will become invalid when the sphere potential exceeds 1.14×10^8 volts. However, for sphere potentials in excess of 10^6 volts, the theory as given above must be modified to include relativistic effects.

A relativistic increase in the mass would manifest itself through the parameter α (Eq. (19)), which is proportional to the mass of the electron. For a given sphere potential, the radius of the current-collection area at infinity would be increased, according to Eq. (25), by a factor $\gamma^{1/3}$ for the Coulomb case, where γ is the ratio of the relativistic mass to the rest mass of the electron. Hence, some relativistic enhancement in current collection (a factor of the order of $\gamma^{2/3}$) may be expected for sphere potentials in excess of 10^6 volts.

The basic defect of the drift approximation theory, as exemplified by Eq. (16), is that conservation of canonical angular momentum has not been taken properly into account. The inclusion of this angular momentum in the theory would result in a reduction of the current-collection area at infinity, since some of the kinetic energy resides in transverse motion, which, due to centrifugal force, tends to keep the electron away from the axis of the system.

The role of canonical angular momentum in limiting the current collection by the sphere will be discussed in the next section.

III. RIGOROUS DYNAMICAL BOUNDS ON CURRENT COLLECTION*

In this section, the integrals of the motion will be analyzed, for an electron moving in a uniform magnetic field which is superimposed on a rotationally symmetric electric field produced by a charged sphere. A relation will be derived which gives, to a good approximation, the shape of the volume of space which contains the trajectory of the electron. The case of interest is that of an electron which enters the volume at infinity, moving initially along a magnetic field line. For a fixed sphere potential, sphere radius, and magnetic field strength, a necessary condition for the electron to be collected is that the inner bounding surface of the containing volume must intersect the sphere. This condition is not sufficient since the electron may "bounce" around within the volume, miss the sphere, and pass out again to infinity. Thus, the question of sufficiency is not easily answered, but the condition of necessity is of interest since it gives an unambiguous lower bound on the sphere potential required to collect current from a given area at infinity. The non-relativistic equations of motion will be considered.

Choose the cylindrical coordinates r, θ, and z to represent the radial, azimuthal, and axial coordinates of the electron, respectively. The z-axis passes through the center of the sphere and is parallel to the magnetic field, of strength B. The Lagrangian of the system may be given by

$$L = \frac{m}{2}\left(\dot{r}^2 + r^2\dot{\theta}^2 + \dot{z}^2 + \omega\dot{\theta}r^2\right) - \Phi(r,z) \qquad (1)$$

where the dots signify time-differentiation, and $\omega \equiv eB/mc$, with e and m representing the charge and mass of the electron, respectively.

* The idea for this analysis is due to B. L. Murphy, of Mt. Auburn Research Associates, whose contributions are gratefully acknowledged.

$\Phi(r,z)$ is the potential energy of the electron, which is as yet an unspecified function of r and z. From this Lagrangian, we may derive the equations of motion, which yield the following first integral:

$$\dot{r}^2 + \dot{z}^2 = \dot{r}_0^2 + \dot{z}_0^2 + c^2\left(\frac{1}{r_0^2} - \frac{1}{r^2}\right) + \omega^2/4\,(r_0^2 - r^2)$$

$$+ \frac{2}{m}\left[\Phi(r_0, z_0) - \Phi(r, z)\right] \tag{2}$$

where

$$c = r_0^2\left(\dot{\theta}_0 + \frac{\omega}{2}\right) \tag{3}$$

and the zero subscripts refer to the initial position of the electron. The constant c is the canonical angular momentum divided by m. Let us assume that the electron starts at infinity, where $\Phi(r_o,z_o)$ vanishes, and has negligible initial kinetic energy, that is, total energy, at infinity. Thus, we set $\dot{r}_o = \dot{\theta}_o = \dot{z}_o = 0$, which simplifies the algebra without changing the essential character of the problem. Thus, Eqs. (2) and (3) lead to the following condition for which $\dot{r} = 0$:

$$\left(\frac{r}{r_0} - \frac{r_0}{r}\right)^2 = \frac{4}{\omega^2 r_0^2}\left[-\frac{2}{m}\Phi(r, z) - \dot{z}^2(r, z)\right] \tag{4}$$

The relation between r and z given by Eq. (4) expresses the equation of the boundary surface of the volume or "bottle" in r-z space containing the electron trajectory.

Several conclusions may be drawn from Eq. (4). There is no real solution unless $\bar{\Phi}$ is negative. In the limit as $\bar{\Phi} \to 0$ or $B \to \infty$, the right-hand-side of Eq. (4) vanishes. Then r approaches its initial value r_o.

Consider the left-hand-side of Eq. (4) as a function of r. It vanishes at $r = r_o$ (the initial value) and rises monotonically to infinity either as r/r_o approaches zero or as r/r_o approaches infinity. That is, it may be considered to have two monotonic branches, one corresponding to $r/r_o < 1$ and one corresponding to $r/ro > 1$.

Now assume that the right-hand-side is positive for all finite z and r, and that the partial derivatives of the right-hand-side with respect to z and r are negative. That is, the right-hand-side is assumed to be a monotonic decreasing function of z with r fixed, and a monotonic decreasing function of r with z fixed. Then, for any fixed value of z, Eq. (4) has two roots, r_{min} and r_{max}, where $r_{min} < r_o$ and $r_{max} > r_o$. Moreover, $r_{min}(z)$ decreases and $r_{max}(z)$ increases, as z decreases. The functions $r_{min}(z)$ and $r_{max}(z)$ define the walls of the "bottle" in r-z space which contains the trajectory of the electron. Figures 4, 6 and 8 illustrate typical bottle shapes. At $z = \infty$, the walls coincide at the radial value r_o, i.e., the bottle collapses to a cylindrical shell, which may be called the initial "magnetic shell." As z goes from ∞ to 0, the inner wall moves inward, and the outer wall moves outward, from the initial radius r_o. At $z = 0$, the inner wall achieves its innermost radius $r_{min}(0)$, while outer wall achieves its outermost radius $r_{max}(0)$. If $r_{min}(0) > a$, where a is the radius of the sphere, the electron trajectory cannot intersect the sphere. Thus, a necessary condition for electron collection is that $r_{min}(0)$ be less than or equal to a.

It is not possible, without knowing z as a function of r and z, to obtain $r_{min}(0)$. We do not know the behavior of $\dot{z}$ since we do not know the analytic behavior of the trajectory. The question

arises whether a useful lower bound for $r_{min}(0)$ can be obtained in the absence of such information. The answer is affirmative, as may be seen by considering the right-hand-side of Eq. (4). If we set $\dot{z}$ to zero, we incur the following consequences: The right-hand-side, under the conditions of the preceding paragraph, is thereby increased in value. The root at r_{min} becomes smaller, and the root at r_{max} becomes greater. That is, the inner wall of the bottle moves further inward and represents a lower bound on $r_{min}(0)$. It is this lower bound which proves to be useful, since the potential distributions of interest are expected to satisfy the conditions of the preceding paragraph. This applies to any spherically symmetric potential, and to axially symmetric potentials which have reasonably smooth behavior.

In order to illustrate the consequences of the bound on $r_{min}(0)$ obtained by setting z = 0 in Eq. (4), we will assume an attractive Coulomb potential distribution in the vicinity of the sphere, in the form:

$$\Phi(r,z) = -\frac{\Phi_0 a}{\sqrt{r^2+z^2}} \qquad \Phi_0 > 0 \tag{5}$$

In Eq. (5), Φ_0 is the magnitude of the potential energy of an electron on the surface of the sphere, and a is the sphere radius. It is convenient to write z as a function of r, using Eqs. (4) and (5). The result, giving the shape of the walls of the bottle, may be put in the form:

$$z^2 = r^2\left[\frac{64}{9}\alpha^2\frac{\frac{r^2}{a^2}}{\left(\frac{r_0^2}{a^2}-\frac{r^2}{a^2}\right)^4} - 1\right] \tag{6}$$

where α is the parameter defined by Eq. (19) of Sec. II. It is repeated here for convenient reference, as follows:

$$\alpha \equiv \frac{3\Phi_0}{m\omega^2 a^2} = 1.71\times10^{-3}\frac{V(\text{volts})}{[a(\text{meters})]^2[B(\text{gauss})]^2} \tag{7}$$

From Eq. (6), the relation between $r_{min}(0)/a$ and r_o/a may be written:

$$\frac{r_o^2}{a^2} = \frac{r_{min}^2(0)}{a^2} + \sqrt{\frac{8}{3}\alpha\frac{r_{min}(0)}{a}} \tag{8}$$

Thus, the condition that $r_{min}(0)$ be less than or equal to a is equivalent to the statement:

$$\frac{r_o^2}{a^2} \leq 1 + \sqrt{\frac{8}{3}\alpha} \tag{9}$$

Therefore, the current collected by the sphere cannot be enhanced by a factor greater than that given by the right-hand-side of Eq. (9), which constitutes a rigorous upper bound.

In order to enhance the current collection by a factor of 100, α must be at least as great as 3.75×10^3. For a sphere radius of 1.5 meters and a magnetic field strength of 0.45 gauss, this means that the sphere potential must be greater than 267α, or 10^6 volts. This is an order of magnitude greater than the value 2×10^5 volts given by the drift theory (Sec. II) for the same enhancement in current. The discrepancy is due to the fact that the conservation of angular momentum, when properly taken into account, causes some of the kinetic energy to appear in transverse motion, thus setting up a centrifugal barrier which tends to keep the electron away from the axis.

It is interesting that the bound given by Eq. (9) is independent of the <u>form</u> of the potential, but depends only on the <u>value</u>

of the potential on the sphere. This may be taken to indicate that shielding has little or no effect on the results of this section. For large sphere potentials, the current collection area at infinity is proportional to $V^{1/2}$, according to Eq. (9), as compared with $V^{2/n+2}$ given by the drift theory (Sec. II). In either case, it is very insensitive to the value and form of the potential.

In the next section, exact trajectory calculations will be presented, which demonstrate the utility of the above analysis.

IV. EXACT TRAJECTORY CALCULATIONS

Assuming that an electron is subjected simultaneously to a uniform magnetic field and a Coulomb electric field generated by a charged sphere, a number of electron trajectories were computed with high precision. A predictor-corrector code was developed for this purpose, with double precision to control round-off errors, and with automatic control of step size which kept the truncation error per step to within an adjustable range.[16] The program was run on an IBM 7094 computer, maintaining a range 10^{-8} to 10^{-10} for the truncation error. It was found that this gave satisfactory accuracy (no significant change with further reduction in step size) without requiring excessive computer time (several minutes for trajectories with many loops).

According to the theory of the drift approximation (Sec. II), a sphere of radius 1.5 meters, immersed in a magnetic field of strength 0.45 gauss, and charged to a potential of 1.29×10^7 volts (a value higher than the values discussed in Sec. II), will collect electron current from an area at infinity 1600 times as great as its own cross-sectional area. On the other hand, the dynamical analysis of Sec. III indicates that the collection area at infinity will not be greater than 360 times the sphere cross-sectional area. The radius of this limiting collection area is 2850 cm.

The trajectory code was employed to study the path of an electron as it comes toward the sphere, starting from infinity with zero energy and moving along a given magnetic field line (defining a cylindrical magnetic shell). Since the numerical calculation must start at a finite point, the initial position was taken at a sufficiently great axial distance from the sphere that the ExB drift would be small. That is, the transverse drift velocity of the guiding center would be less than the mean thermal velocity of the electron at infinity, while the longitudinal velocity would be appropriate to an electron of zero total energy. For a sphere potential of 1.29×10^7 volts, a sphere radius 1.5 meters, a magnetic

field of 0.45 gauss, a temperature of 0.129 volts, and magnetic shells of radius 50 meters or less, the required axial starting position is 50,000 cm from the sphere. For all the runs discussed here, the axial starting position was fixed at 50,000 cm.

Several runs were made with varying magnetic shell radii. According to the analysis of Sec. III, the radius of the limiting collection area is 2850 cm, under the conditions stated. Runs were made with starting shell radii both greater than and less than 2850 cm. In both cases, the limiting surfaces ("bottles") in r-z space were found to represent well the shape of the actual space containing the trajectories. The trajectories computed with starting radii less than 2850 cm were more interesting than those with greater radii, since the electron made many close passes to the sphere.

The trajectories with starting radii of 2850 cm, 1500 cm, and 1000 cm will be discussed in some detail here. Figures 4, 6, and 8 show the outer and inner surfaces of the bottles in r-z cylindrical space containing the trajectories of electrons starting at radii 2850 cm, 1500 cm, and 1000 cm, respectively. The spatial extent covered in the z-direction is 100,000 cm. Figures 5, 7, and 9 show close-up views of the inner surface of the bottle, in the vicinity of the sphere, for the cases of initial radii 2850 cm, 1500 cm, and 1000 cm, respectively. In all cases, the electron tended to oscillate between positive and negative values of z, while oscillating very frequently in r and bouncing off the walls of the confining bottle. The trajectories were arbitrarily terminated when they reached $z = \pm 100{,}000$ cm. The trajectories are too complicated to depict in drawings, but their features will be described.

Tables II, III, and IV show the successive minima and maxima attained in the z-direction by the electron trajectory in the cases of 2850 cm, 1500 cm, and 1000 cm, respectively. The confinement

effect is most marked in the 2850-cm case (Table II), in which the electron oscillates 15 times in the z-direction before passing out of the plane at z = 100,000 cm. Superimposed on each of these oscillations are many oscillations in the r-direction. The curves marked by the numerals 1, 2, and 3 in Fig. 5 are portions of the 2850-cm trajectory in the vicinity of the sphere. They are associated with the extrema at z = 441 cm, -707 cm, and -383 cm, respectively. These extrema are also indicated in Table II by the same numerals, showing that they occur after 5 oscillations, 9 oscillations, and 12 oscillations, respectively, in the z-direction.

The 1500-cm trajectory oscillates 4 times in the z-direction before passing out of the plane at z = 100,000 cm. The curves marked by the numerals 1, 2, and 3 in Fig. 7 are portions of this trajectory in the vicinity of the sphere. They are associated with the extremum at z = -372 cm, the portion between the extrema z = 6147 cm and -4916 cm, and the extremum at z = -598 cm, respectively. These extrema are indicated in Table III. Since the space in which the trajectory was followed was limited, it is possible that, after many more oscillations in a larger space, the electron would return and strike the sphere.

The 1000-cm trajectory oscillates 3½ times, after which the electron strikes the sphere. The curves marked by the numerals 1, 2, and 3 in Fig. 9 are portions of this trajectory in the vicinity of the sphere. The numerals 1 and 2 are associated with the extrema at z = -160 cm and -523 cm, respectively. The numeral 3 denotes the final portion which intersects the sphere. These portions are indicated in Table IV.

It is interesting to observe, in Figs. 5, 7, and 9, how close the trajectory comes to the inner wall of the bottle. This illustrates rather dramatically the sharpness of the analytical bounds derived in Sec. III. However, it is evident that an electron which is permitted to hit the sphere on the basis of these bounds

may spend a great deal of time in the vicinity of the sphere.

This section completes the treatment of current collection at large potentials, which comprises the material of Part I of this report.

PART II

ELECTRON COLLECTION AT SMALL POTENTIALS

Sec. V General Method for Self-Consistent Solution

Sec. VI Calculations with Spherical Symmetry

Sec. VII One-Dimensional Model for Density

V. GENERAL METHOD FOR SELF-CONSISTENT SOLUTION

Assume that the sphere is immersed in a collision-free plasma of electrons and positive ions, where T is the temperature of the plasma, n_o is the normal particle density of ions and electrons in the ambient plasma, and the velocity distributions in the ambient plasma are assumed to be Maxwellian. There is a uniform magnetic field, the presence of which does not affect the velocity distributions in the undisturbed plasma at "infinity." The calculation of the current collected by the sphere for a given sphere potential requires the solution of a set of simultaneous equations, including a Poisson equation in which the charge density depends on the behavior of the densities in phase space. These densities are themselves solutions of the collision-free Boltzmann equation (which need not be written down here) and are constant along trajectories of constant total energy. The complete set of equations to be solved simultaneously will now be presented, and these will be followed by a detailed explanation. The equations are:

$$\nabla^2 \phi = \frac{n_e}{n_o} - \frac{n_i}{n_o} \tag{1}$$

$$\frac{n_e(\vec{r})}{n_o} = \iiint_{\text{occupied}} f_e(\vec{r}, \vec{v}_e)\, d^3\vec{v}_e \tag{2}$$

$$\frac{n_i(\vec{r})}{n_o} = \iiint_{\text{occupied}} f_i(\vec{r}, \vec{v}_i)\, d^3\vec{v}_i \tag{3}$$

$$f_e = \frac{1}{\pi^{3/2}} e^{\phi} e^{-v_e^2} \tag{4}$$

$$f_i = \frac{1}{\pi^{3/2}} e^{-\phi} e^{-v_i^2} \tag{5}$$

$$I_e = e n_o \sqrt{\frac{2kT}{m_e}} \underset{\text{Surface}}{\iint} \vec{d^2\Sigma} \cdot \underset{\text{occupied}}{\iiint} f_e \vec{v_e} \, \vec{d^3 v_e} \tag{6}$$

$$I_i = e n_o \sqrt{\frac{2kT}{m_i}} \underset{\text{surface}}{\iint} \vec{d^2\Sigma} \cdot \underset{\text{occupied}}{\iiint} f_i \vec{v_i} \, \vec{d^3 v_i} \tag{7}$$

$$I = I_i - I_e \tag{8}$$

In Eq. (1), The Poisson equation, ϕ denotes the electrostatic potential energy of an ion and $-\phi$ denotes the electrostatic potential energy of an electron, in units of kT. All lengths are taken in units of the Debye length, $(kT/4\pi n_o e^2)^{1/2}$. The solution of Eq. (1) is subject to the boundary conditions that ϕ must have the value ϕ_o on the surface of the sphere, and must vanish at infinity. In Eqs. (2) and (3), the fractional particle densities of electrons and ions relative to their values at infinity are denoted by n_e/n_o and n_i/n_o, respectively, and are functions of the local position vector $\vec{r}$. The densities are given by integrals over local velocity space of certain functions, where $\vec{v}_e$ and $\vec{v}_i$ denote the local velocity vectors of an electron and an ion, respec-

tively, at the point $\vec{r}$. The electron velocity v_e and the ion velocity v_i are taken to be in units of $(2kT/m_e)^{1/2}$ and $(2kT/m_i)^{1/2}$, respectively, where m_e and m_i denote the masses of an electron and an ion, respectively. In the integral of Eq. (2), each value of $\vec{v}_e$ characterizes a trajectory, along which the density in phase space is constant. Thus, the integrand of Eq. (2) vanishes when the trajectory is unoccupied, i.e., when it corresponds to an electron which comes to $\vec{r}$ from a non-emitting surface. The integrand of Eq. (2) is given by Eq. (4) when the trajectory corresponds to an electron which comes to $\vec{r}$ from infinity, that is, the trajectory is occupied. Similar considerations apply to the ion density, given by Eqs. (3) and (5). In Eqs. (6) and (7), I_e and I_i are the currents of electrons and ions, respectively, collected by the sphere, and in Eq. (8), I is the net current collected by the sphere. In Eq. (6) or Eq. (7), the current density vector is given by a triple integral over velocity space, and its normal component is integrated over the surface of the sphere. The current density integrals have contributions only from occupied trajectories, and these contributions are given by Eqs. (4) and (5), similar to the density integrals in Eqs. (2) and (3).

It will be assumed that charged particles incident on the surface of the sphere are absorbed. The sphere is also assumed to emit a given current of electrons. If the emitted electrons were to contribute to the charge density, this contribution would appear in the integrand of Eq. (2). If any of the emitted electrons were to return to the sphere, the contribution of this current could appear in the integrand of Eq. (6). However, it will be assumed that the emitted electrons are ejected at such a high velocity that their density contribution is negligible and that they do not return to the sphere.

The self-consistent solution desired is the solution of Eqs. (1) - (5), for a given potential ϕ_o on the sphere. When this has been achieved, the evaluation of Eqs. (6) - (8) gives the corresponding collected current. A computational procedure for the solution of Eqs. (1) - (5) is the following.

The space in the vicinity of the sphere may be represented by a grid of points such as that shown in Fig. 10. Since the problem is axially symmetric about the direction of the magnetic field, a spherical polar coordinate system has been chosen. The grid is shown to be rectangular in R, the spherical radial distance, and θ, the polar angle. The magnetic field direction corresponds to $\theta = 0$. The sphere surface, R_o, is represented by the first row of points in the grid. The problem is also symmetric about the equatorial plane at $\theta = \pi/2$.

The potential and density are defined as functions of position on the points of this grid. If the magnetic field were non-uniform, it also could be specified on the same grid. The potential assumes the value ϕ_o on the bottom row of points, i.e., $R = R_o$. The potential is assumed to vanish on the top row of points, at $R = R_{max}$, which will be called "the boundary." The choice of the proper value of R_{max} is a difficult matter, as discussed in Sec. I (Introduction). It must be far enough out to satisfy the requirement that its position does not affect the potential in the region of interest. Putting it out too far renders the solution difficult to obtain. This matter will be considered further in Sec. VI.

In Eq. (1), the Poisson equation, the Laplacian differential operator may be approximated by a difference operator defined with respect to the given grid. Let the grid points be characterized by the two indices, i and j, where i refers to the radial coordinate and j refers to the angular coordinate.

Then the Poisson equation, in difference form, may be expressed by the following possible scheme:

$$C(i,j+1)\,\phi(i,j+1) + C(i,j-1)\,\phi(i,j-1)$$

$$+ C(i+1,j)\,\phi(i+1,j) + C(i-1,j)\,\phi(i-1,j)$$

$$+ C(i,j)\,\phi(i,j) = F(i,j) \qquad (9)$$

Equation (9) expresses a linear relation between the potential at the (i,j)-th grid point and nearest vertical and horizontal neighbors. The function F(i,j) on the right-hand-side is the difference between $n_e(i,j)$ and $n_i(i,j)$, i.e., the electron and ion particle densities at the (i,j)-th grid point.

The set of Eqs. (9) for all interior grid points, together with equations of symmetry at grid points on the axis $\theta = 0$, constitute a set of simultaneous non-linear equations for the potentials at the grid points.[15]

A fundamental difficulty, aside from the question of stability associated with the position of the boundary where the potential vanishes, is that of the evaluation of the right-hand-side of Eq. (9), i.e., of F. This function cannot be expressed analytically in general, and depends, not only on the local value of the potential, but also on the potential at other points. That is, the values of n_e and n_i are affected by the missing contributions of particles which cannot get to the (i,j)-th grid point from other parts of space. Thus, n_e or n_i must be evaluated by performing the triple integrals in velocity space, Eqs. (2) and (3), numerically, where each evaluation of the integrand requires the calculation of a

trajectory. Since the integrands are either zero or the analytic functions given by Eqs. (4) and (5), the essential function of the numerical approach is to determine the occupied domain in velocity space. The numerical evaluation of a triple integral, such as Eq. (2) or (3), consists in replacing it by an approximating triple quadrature of the form:

$$n(i,j) = \sum_{k}^{N_1} \sum_{\ell}^{N_2} \sum_{n}^{N_3} A(k,\ell,n)\, f(i,j,k,\ell,n) \qquad (10)$$

where the triplet of indices (k, ℓ, n) refers to the velocity vector $\vec{v}(k,\ell,n)$ which defines the (k, ℓ, n)-th trajectory. Equation (10) is sometimes called a "sum over trajectories." The function $f(k, \ell, n)$ is evaluated by tracing the (k, ℓ, n)-th trajectory backwards in time to its source. If the source is a point at "infinity", i.e., on the boundary of the grid, f is given by Eq. (4) for an electron and by Eq. (5) for an ion. If the source is found to be on the surface of the sphere, f is set to zero. (If emission of particles from the sphere surface were to be taken into account, f would be assigned an appropriate value at this point.) The coefficient $A(k, \ell, n)$ depends on the quadrature scheme (e.g., Gaussian). The accuracy of the trajectory sum in Eq. (10) may be increased by increasing the product $N_1N_2N_3$, i.e., the number of trajectories.

Each term in the trajectory sum requires the calculation of a trajectory. Starting at the (i,j)-th grid point with an initial velocity $\vec{v}(k, \ell, n)$, the equations of motion may be integrated backwards in time, using any of several methods, such as a predictor-corrector, a Runge-Kutta, or a Taylor series method. The potential gradient at any position in the grid may be obtained by interpolation. The same grid may be used for both ions and electrons by reversing the signs of the potentials.

The self-consistent solution of Eq. (9) is the set of potentials at the grid-points, which may be considered as the components of a vector $\vec{\phi}$. We may express the problem formally as that of solution of the matrix equation:

$$L\vec{\phi} = \vec{F}(\vec{\phi}) \tag{11}$$

where L is a matrix operator and $\vec{F}$ is a vector, whose component at the (i,j)-th grid point depends on the values of ϕ at all grid points. Since, as discussed above, $\vec{F}$ cannot be expressed analytically as a function of $\vec{\phi}$, an iteration procedure appears to be the only recourse. A possible iteration procedure would be the following:

$$L\vec{\phi}^{p} = \vec{F}(\vec{\phi}^{p-1}) \tag{12}$$

where $\vec{\phi}^{p}$ denotes the p-th iterate for $\vec{\phi}$. The implication of Eq. (12) is that one begins with a guess for $\vec{\phi}$ and evaluates the sum Eq. (10) at all grid points, for both electrons and ions, in order to obtain a vector $\vec{F}$. Eq. (12) is then solved as a set of linear equations for $\vec{\phi}$, which becomes in turn the next iterate. There are two questions which arise in connection with this procedure. One is concerned with whether the procedure will converge. The other is concerned with the accuracy of the solution when convergence is achieved. The answers to these questions are related to each other. Since the true solution cannot be known, confidence in the correctness of the solution obtained is gained by observing whether it is sensitive to the numerical parameters. These parameters include the number of grid points, the spatial extent of the grid, the number of trajectories per grid point, and the accuracy of individual trajectories. The convergence of the procedure is connected with the stability of the iteration procedure, which in turn appears to depend more strongly on the spatial extent of the

grid than on any other parameter. Numerical experiments discussed in Sec. VI, using the program described above, bear out this assertion. (See also Reference 13). There is a tendency for the solution to become insensitive to the boundary position as this position is moved outward. However, beyond a certain position convergence cannot be obtained. Thus, as the boundary is moved progressively outward, one hopes to observe the insensitivity before divergence sets it. This does not necessarily occur. However, convergence can be always assured at the expense of accuracy by moving the boundary inward.

In the next section, numerical experiments on convergence and stability will be described.

VI. CALCULATIONS WITH SPHERICAL SYMMETRY

This section deals with numerical solutions to the Poisson equation

$$\nabla^2 \phi = F \tag{1}$$

Let r and θ represent the radius and polar angle in a spherical polar coordinate system. In this coordinate system, Eq. (1) can be written:

$$\frac{\partial^2 \phi}{\partial r^2} + \frac{2}{r}\frac{\partial \phi}{\partial r} + \frac{1}{r^2}\left[\cot\theta \frac{\partial \phi}{\partial \theta} + \frac{\partial^2 \phi}{\partial \theta^2}\right] = F(r,\theta) \tag{2}$$

It is convenient to transform from the variable ϕ to the variable $\psi \equiv r\phi$, where ψ satisfies the equation

$$\frac{\partial^2 \psi}{\partial r^2} + \frac{1}{r^2}\left[\cot\theta \frac{\partial \psi}{\partial \theta} + \frac{\partial^2 \psi}{\partial \theta^2}\right] = r F(r,\theta) \tag{3}$$

The formulation of Eq. (3) was found to have better numerical properties than Eq. (2) when difference analogues were used with unequal spacing. For a grid in the form of that shown in Fig. 10, the following difference analogue, centered about the (i,j)-th grid point, was adopted:

$$C(i+1,j)\,\psi(i+1,j) + C(i-1,j)\,\psi(i-1,j)$$

$$+ C(i,j+1)\,\psi(i,j+1) + C(i,j-1)\,\psi(i,j-1)$$

$$+ C(i,j)\,\psi(i,j) = r_i F(i,j) \tag{4}$$

where the coefficients are given by

$$C(i+1,j) = \frac{2}{h_2(h_2+h_4)} \tag{5}$$

$$C(i-1,j) = \frac{2}{h_4(h_2+h_4)} \tag{6}$$

$$C(i,j+1) = \frac{1}{\pi^2 r_i^2 h_1(h_1+h_3)}\left[2 + \pi h_3 \cot \pi\theta_j\right] \tag{7}$$

$$C(i,j-1) = \frac{1}{\pi^2 r_i^2 h_3(h_1+h_3)}\left[2 - \pi h_1 \cot \pi\theta_j\right] \tag{8}$$

$$C(i,j) = -\frac{2}{h_2 h_4} - \frac{1}{\pi^2 r_i^2 h_1 h_3}\left[2 + \pi(h_3-h_1)\cot \pi\theta_j\right] \tag{9}$$

$$h_1 = \theta_{j+1} - \theta_j \tag{10}$$

$$h_3 = \theta_j - \theta_{j-1} \tag{11}$$

$$h_2 = r_{i+1} - r_i \tag{12}$$

$$h_4 = r_i - r_{i-1} \tag{13}$$

where θ is in units of π.

Equations (5) - (13) constitute a difference scheme defined on a grid with non-uniform spacing.[15]

In order to study the numerical convergence properties of the Poisson calculation, problems with spherical symmetry were investigated. Moreover, since the calculation of particle densities required more computer time than any other phase of the calculation, it was decided provisionally to represent the space charge density function on the right-hand-side of the Poisson equation with an analytical model function. The convergence properties of the numerical scheme should not depend strongly on the exact nature of the space charge function. The analytic model function employed is defined as follows:

$$F = K F_o \tag{14}$$

where

$$F_o \equiv \mp\left[\frac{2}{\sqrt{\pi}}\sqrt{|\phi|} + e^{|\phi|}\,\mathrm{erfc}\sqrt{|\phi|}\right] \pm e^{-|\phi|} \tag{15}$$

and

$$K \equiv \frac{1}{2}\left[1 + \sqrt{1 - \frac{r_o^2}{r_2}}\right] \tag{16}$$

where ϕ is the potential energy of an electron in units of kT. The upper signs are to be used in Eq. (15) when ϕ is negative, and the lower signs when ϕ is positive. That is, when ϕ is negative, the electrons are attracted, and the (singly-charged) ions are repelled, the density of ions in this case being given by the exponential term. The factor K is a correction, assuming straight-line trajectories, for the shadowing effect of the sphere, $4\pi K$ being the solid angle subtended at the point r by the sphere. The sphere radius is r_o. The function F_o is obtained by evaluating the density integrals (see Eqs. (2) and (3) of Sec. V) analytically under the assumption that the sphere has no shadowing effect (i.e., the sphere is transparent).

Using the F of Eq. (14), tests were made for a sphere of radius r_o = 150 Debye lengths (Debye length = 1 cm) having potentials ϕ_o = -10 kT and -100 kT (kT = .1294 electron-volts). The solution of the Poisson problem was found to be extremely unstable when the outer boundary of the grid, where ϕ = 0, was set at 5000 cm. The solution became stable when the outer boundary was brought within 157 cm, i.e., to within 7 cm of the sphere surface. This phenomenon is connected with the fact that the net charge density F is small at radii exceeding 157 cm, and that a small net charge density at great distances makes a large contribution to the potential. This is manifested in the Poisson difference equations by the weighting of F in proportion to the radial distance (Eq. (4)). In consequence, the contribution of distance space charges must be carefully taken into account. A numerical limiting process was adopted, in which more and more distant space charges were progressively included, by moving the boundary successively outward in steps and solving a sequence of corresponding problems. The potentials at fixed radii were observed to tend to converge to values independent of the boundary position before the problems became unstable and incapable of solution. The process is illustrated by the following example.

With the sphere potential fixed at -10 kT, a sequence of problems was solved, in which the radius of the outer boundary of the grid was set at the successive values: 152, 153, 154, 155, 156, 157, etc., cm. The Poisson difference equations, Eqs. (4), using Eq. (14) for the right-hand-side, was solved in each case. The solutions are shown in Table V.

The solutions were obtained by an iterative process, in which F = 0 served as the initial guessed input to obtain the zeroth potential iterate (Laplace solution). Successive F-iterates were averaged with preceding ones to form new inputs.

In Table V, the potentials are shown at fixed radial positions in columns, each column representing the solution of a problem with a given boundary position. The position of the boundary for each problem is indicated above the corresponding column. At the head of each column, the notation $\phi(N)$ indicates that N iterations were required to reproduce the potential distribution to three significant figures. Thus, as the boundary moves out, the number of iterations required increases, and the value of the potential at a fixed radius tends to converge. However, when the boundary was at 157 cm, the solution had not converged after 37 iterations. The successive potential iterates oscillated between two distinct "modes". In the column corresponding to 157 cm, the range of oscillation is shown, for each radial position, between the 9th and 10th iterates. These modes were slowly coming together, but it was clear from the rate of convergence that many more iterations would be required. At 158 cm, the oscillation occurred between two modes which diverged rapidly from one another.

The problems with 155 cm or 156 cm probably represent the most accurate solutions in the sequence of problems shown.

Runs were also made with ϕ_o = -100 kT, for which the solution became unstable for boundary positions beyond 158 cm. The solution at 158 cm is shown in Table VI.

The electron-ion density calculation program described in Sec. V was coded for the computer and test runs were made to repeat the sequence of problems discussed above. However, the density values obtained were erratic, due to the use of an insufficient number of trajectories per point when the potential falls off very rapidly with distance. An investigation is under way to determine the required number of trajectories. This has not yet been completed. The same circumstances apply to a current density program coded for the computer. Using 8192 trajectories for the problem with ϕ_o = -10 kT, the solution of which is given in Table V, the current was calculated to be 1.09, in units of $4\pi r_o^2 (kT/2\pi m)^{1/2}$

VII. ONE-DIMENSIONAL MODEL FOR DENSITY

When the ambient magnetic field is strong, an important simplification can be made with respect to calculating the density of electrons, due to the fact that the electric field is rotationally symmetric about an axis parallel to the magnetic field. The magnetic field can be considered "strong" in the sense that the Larmor radius (2.7 cm in the present case) is small compared with the radius of the sphere (150 cm in the present case). The motivation for using a simplified model is that density evaluations, obtained by following many trajectories as outlined in Sec. V, typically require more computer time than other parts of a self-consistent calculation. As the magnetic field increases in strength, the tight spiral motions of the particles require more calculational steps in following their trajectories. On the other hand, the drift approximation becomes increasingly applicable, and, when the magnetic field is very strong, may yield an excellent approximation to the density.

According to the theory of the drift approximation (Sec. II), the electron guiding-centers are essentially constrained to move on the surfaces of cylinders concentric with the axis of the system. The axis is parallel to the magnetic field and passes through the center of the sphere. Assuming that the contribution to the density due to the E x B drift velocity is negligible compared with the contribution due to longitudinal velocities, the density of electrons on the right-hand side of the Poisson equation (Eq. (1) of Sec. V) can be evaluated by a formula based on a one-dimensional model. The assumption that the E x B drift contribution is negligible should be valid if the electric field is not strong. Thus, due to rotational symmetry, the density of particles at a point may be calculated as if the particles which contribute to the density at that point moved on a rigid straight line, passing through that point and parallel to the magnetic field direction. The formula for the density of particles at a point may be derived in the following way.

Let the line of motion be oriented parallel to the z-axis of the rotationally symmetric system of coordinates centered at the sphere. Let the magnetic field lines be separated into two classes, those which intersect the sphere, and those which do not intersect it. These two classes will be discussed separately.

A. INTERSECTING LINE

We will first treat the case of an intersecting field line, assuming that the potential distribution is given by the sample form shown in Fig. 11a. Between the sphere surface at $z = z_o$ and $z = +\infty$ to the right, two peaks are shown, at $z = z_1$ and $z = z_2$. The potential at the sphere surface is ϕ_o, and at z_1 and z_2 the potential is ϕ_1 and ϕ_2, respectively. (The symbol ϕ denotes the potential energy in units of kT.) The peak potential values are shown in the sample as positive, for the purpose of illustrating the method, which is more complicated when there are positive peaks than when the potential is completely negative. There are four intervals to be considered: (z_o, z_1), (z_1, z_3), (z_3, z_2), and (z_2, ∞). (The symbol (z_a, z_b) denotes "the interval between z_a and z_b.") These intervals will be considered as follows.

In the interval (z_o, z_1), there are no particles moving to the right since the sphere absorbs, but does not emit, particles. There are particles moving to the left, which have come from $+\infty$ and have overcome the barrier of height ϕ_1 at $z = z_1$. The density of particles moving to the left (n_L) in the interval (z_o, z_1) is given by the integral (the one-dimensional analogue of Eq. (2) of Sec. V) in one-dimensional velocity space:

$$n_L = \frac{e^{-\phi}}{\sqrt{\pi}} \int_{\sqrt{\phi_1 - \phi}}^{\infty} e^{-v^2} dv = \frac{e^{-\phi}}{2} \operatorname{erfc} \sqrt{\phi_1 - \phi} \qquad (1)$$

where the lower limit of the integration is the minimum velocity (in units of $\sqrt{2kT/m}$) which a particle can have in (z_o, z_1) after surmounting the peak ϕ_1. The symbol erfc (x) denotes the complementary error function of x. Since the density of particles moving to the right (n_R) is zero, the density of particles in (z_o, z_1) is

$$n = n_L + n_R = \frac{e^{-\phi}}{2} \operatorname{erfc} \sqrt{\phi_1 - \phi} \tag{2}$$

The intervals (z_1, z_3) and (z_2, ∞) are equivalent. In these intervals, particles moving to the left have a minimum velocity of zero and a maximum velocity of infinity, while those moving to the right have a minimum velocity of zero and a maximum velocity of $\sqrt{\phi_1 - \phi}$. The latter particles are those which are reflected from the top of the peak at ϕ_1. Thus,

$$n_L = \frac{e^{-\phi}}{\sqrt{\pi}} \int_0^{\infty} e^{-v^2} dv \tag{3}$$

$$n_R = \frac{e^{-\phi}}{\sqrt{\pi}} \int_0^{\sqrt{\phi_1 - \phi}} e^{-v^2} dv \tag{4}$$

so that the density in (z_1, z_3) or (z_2, ∞) is:

$$n = n_L + n_R = e^{-\phi} \left[1 - \frac{1}{2} \operatorname{erfc} \sqrt{\phi_1 - \phi} \right] \tag{5}$$

The interval (z_3, z_2) is more complicated than the others, since there are peaks on both sides of the point of interest. In this interval, particles moving to the left have a minimum velocity of $\sqrt{\phi_2 - \phi}$ and a maximum velocity of infinity, while those moving to the right have a minimum velocity of $-\sqrt{\phi_2 - \phi}$ and a maximum velocity of $\sqrt{\phi_1 - \phi}$. Thus,

$$n_L = \frac{e^{-\phi}}{\sqrt{\pi}} \int_{\sqrt{\phi_2 - \phi}}^{\infty} e^{-v^2} dv \tag{6}$$

$$n_R = \frac{e^{-\phi}}{\sqrt{\pi}} \int_{\sqrt{\phi_2 - \phi}}^{\sqrt{\phi_1 - \phi}} e^{-v^2} dv \tag{7}$$

so that the density in (z_3, z_2) is:

$$n = n_L + n_R = e^{-\phi} \left[\operatorname{erfc} \sqrt{\phi_2 - \phi} - \frac{1}{2} \operatorname{erfc} \sqrt{\phi_1 - \phi} \right] \tag{8}$$

This expression is based on the assumption that the peak ϕ_1 is higher than the peak ϕ_2. That is, for this interval, ϕ cannot be greater than the lower of the two peaks, and in this interval has values less than or equal to ϕ_2.

If the peak ϕ_1 had been lower than the peak ϕ_2, it would have been necessary to define an interval (z_1, z_3) (not shown in Fig. 11a) in which ϕ would have values less than or equal to ϕ_1. Then n_R would be zero instead of Eq. (7), and the density would be given by

$$n = \frac{e^{-\phi}}{2} \operatorname{erfc} \sqrt{\phi_2 - \phi} \qquad (9)$$

rather than by Eq. (8).

The rules for obtaining Eqs. (1) - (9) can be generalized by considering the following three categories, which exhaust all cases, for a given position z where the potential has the value ϕ. It is assumed that there is a highest peak of value ϕ_p greater than any other peak in the potential distribution, and that this value is greater than or equal to zero. There may be secondary peaks of value greater than or equal to zero. Thus:

1. The peak ϕ_p lies between z and ∞ (to the right). In this case, the density is given by:

$$n = \frac{e^{-\phi}}{2} \operatorname{erfc} \sqrt{\phi_p - \phi} \qquad (10)$$

2. The peak ϕ_p lies between z and z_o (to the left), and the highest peak between z and ∞ (to the right) has a value $\phi_q < \phi$. In this case, the density is given by:

$$n = e^{-\phi} \left[1 - \frac{1}{2} \operatorname{erfc} \sqrt{\phi_p - \phi} \right] \qquad (11)$$

3. The peak ϕ_p lies between z and z_o (to the left), and the highest peak between z and ∞ (to the right) has a value $\phi_q > \phi$. In this case, the density is given by:

$$n = e^{-\phi}\left[\operatorname{erfc}\sqrt{\phi_q - \phi} \;-\; \frac{1}{2}\operatorname{erfc}\sqrt{\phi_p - \phi}\right] \quad (12)$$

A few important examples of the application of Eqs. (10) - (12) are the following ones. If (see Fig. 12a) the potential falls monotonically from the positive value ϕ_o (at z_o) to zero (at ∞), the highest peak is $\phi_p = \phi_o$ (at z_o) and Eq. (11) is the appropriate equation. If (see Fig. 12b) the potential rises monotonically from the negative value $-\phi_o$ (at z_o) to zero (at ∞), the highest peak is $\phi_p = 0$ (at ∞), and Eq. (10) is the appropriate equation. If (see Fig. (12c) the potential falls from the positive value ϕ_o (at z_o) to zero (at z_1), attains a negative minimum value $-\phi_m$, and then rises to zero (at ∞), the highest peak is $\phi_p = \phi_o$ (at z_o). For $z < z_1$, the highest peak in the range between z and ∞ (to the right) is $\phi_q = 0 < \phi$, and Eq. (11) is the appropriate equation. For $z > z_1$, the highest peak in the range between z and ∞ (to the right) is $\phi_q = 0 > \phi$, and Eq. (12) is the appropriate equation. If (see Fig. 12d) the potential rises from the negative value $-\phi_o$ (at z_o) to zero, attains a positive maximum value ϕ_m (at z_m), and then falls to zero (at ∞), the highest peak is $\phi_p = \phi_m$ (at z_m). For $z < z_m$, ϕ_p is to the right, and Eq. (10) is the appropriate equation. For $z > z_m$, ϕ_p is to the left, and the highest peak in the range between z and ∞ (to the right) is $\phi_q = 0 < \phi$, and Eq. (11) is the appropriate equation.

This completes the discussion of the case of an intersecting field line.

B. NON-INTERSECTING LINE

We will now treat the case of a non-intersecting field line, assuming that the potential distribution is given by the sample form shown in Fig. 11b. This case is simpler than that of an intersecting line. The potential distribution is assumed to be symmetric about z = 0, which corresponds to the equatorial plane of the sphere. Referring to Fig. 11b: In the interval $(0, z_1)$, electrons coming from $z = \pm\infty$ have a minimum velocity of magnitude $\sqrt{\phi_1 - \phi}$, so that the density is given by

$$n = \frac{2}{\sqrt{\pi}} e^{-\phi} \int_{\sqrt{\phi_1-\phi}}^{\infty} e^{-v^2} dv = e^{-\phi} \operatorname{erfc} \sqrt{\phi_1-\phi} \qquad (13)$$

In the intervals (z_1, z_3) and (z_2, ∞), electrons coming from $z = \pm\infty$ have a minimum velocity of zero, so that the density is given by

$$n = e^{-\phi} \qquad (14)$$

In the interval (z_3, z_2), electrons coming from $z = \pm\infty$ have a minimum velocity of magnitude $\sqrt{\phi_2 - \phi}$, so that the density is given by

$$n = e^{-\phi} \operatorname{erfc} \sqrt{\phi_2-\phi} \qquad (15)$$

The rules for obtaining Eqs. (13) - (15) may be generalized by considering the following two categories:

1. There is a peak ϕ_p, of value greater than or equal to zero, in the interval (z, ∞), such that $\phi_p > \phi$. In this case, the density is given by:

$$n = e^{-\phi} \operatorname{erfc} \sqrt{\phi_p - \phi} \qquad (16)$$

2. There is no potential of value greater than ϕ in the interval (z, ∞). In this case, the density is given by:

$$n = e^{-\phi} \qquad (17)$$

As in the case of the intersecting line, the peak ϕ_p may be the zero potential at infinity.

This completes the derivation of the one-dimensional formulae for the density of electrons. If the sphere is large compared with the Larmor radius of ions, the above formulae would apply to the ions as well. In applying these formulae to the self-consistent problem of a spherical probe in a magnetic field, it would be convenient to use cylindrical coordinates so that the particle density can be evaluated on shells of constant cylindrical radius, employing the formulae of this section.

TABLE I

Drift Equation Solutions for Coulomb Potential.
Collection radius at infinity = r_∞. Sphere radius = a.
Sphere radius 1.5 meters. Magnetic field 0.45 gauss.

V (volts)	$\alpha^{1/3}$	(r_∞/a)	$(r_\infty/a)^2$
1	.155	1.00125	1.0025
10	.335	1.0124	1.025
10^2	.720	1.1161	1.246
10^3	1.55	1.763	3.107
10^4	3.35	3.685	13.58
10^5	7.20	7.932	62.92
10^6	15.5	17.09	292.0
10^7	33.5	36.82	1355
10^8	72.0	79.32	6303

TABLE II

Trajectory Extrema. r_∞ = 2850 cm.
Sphere Potential 1.29×10^7 volts.
Sphere Radius 150 cm. Magnetic Field 0.45 gauss.

	z (cm)		z (cm) (continued)	
	50000		-21725	
	-1602		1635	
	2995		-10222	
	-38796		4479	
	8375	(2)	- 707	
	- 2684		48062	
	8141		-8362	
	-50874		2219	
	6143		-13218	
	-27700		24134	
(1)	441	(3)	- 383	
	- 5863		23989	
	3684		13540	
	- 4981		801	
	2406		-65714	
			100000	(out of region)

TABLE III

Trajectory Extrema. r_∞ = 1500 cm.
Sphere Potential 1.29 x 10^7 volts.
Sphere Radius 150 cm. Magnetic Field 0.45 gauss.

	z (cm)	
	50000	
(1)	- 372	
	18016	
	-7642	
	6147	
(2)	-4916	
	21463	
(3)	- 598	
	100000	(out of region)

TABLE IV

Trajectory Extrema. r_∞ = 1000 cm.
Sphere Potential 1.29 x 10^7 volts.
Sphere Radius 150 cm. Magnetic Field 0.45 gauss.

	z (cm)	
	50000	
(1)	- 160	
	42546	
(2)	- 523	
	50329	
	-1142	
	10301	
	-5075	
(3)	- 84	(hit)

TABLE V

Poisson Solution. Spherical Symmetry.

ϕ_o = -10 (1.29 volts). Sphere Radius 150 cm.

Boundary at	152	153	154	155	156	157 cm.
Radius (cm)	$\phi(5)$	$\phi(7)$	$\phi(9)$	$\phi(9)$	$\phi(11)$	$\phi(9/10)$*
150	-10	-10	-10	-10	-10	-10 / -10
151	- 4.3	- 5.3	- 5.49	- 5.54	- 5.55	-5.8 / -5.4
152	0	- 2.1	- 2.6	- 2.73	- 2.75	-3.2 / -2.4
153		0	- 1.0	- 1.16	- 1.19	-1.8 / -0.8
154			0	- 0.39	- 0.49	-1.1 / +0.03
155				0	- 0.15	-0.8 / +0.3
156					0	-0.4 / +0.2
157						0 / 0

$\phi(n)$ denotes potential after n iterations.

* Not converged after 37 iterations. Showing 9th/10th iterates.

TABLE VI

Poisson Solution. Spherical Symmetry.

ϕ_o = -100 (12.9 volts). Sphere Radius 150 cm.

Boundary at	155	156	157	158 cm.
Radius (cm)	$\phi(6)$	$\phi(8)$	$\phi(15)$*	$\phi(15)$*
150	-100	-100	-100	-100
151	- 70.5	- 71.8	-72.4	- 72.7
152	- 46.7	- 49.4	- 50.6	- 51.1
153	- 27.7	- 31.8	- 33.7	- 34.5
154	- 12.5	- 18.4	- 21.0	- 22.0
155	0	- 8.1	- 11.7	- 13.1
156		0	- 4.9	- 6.9
157			0	- 2.8
158				0

$\phi(n)$ denotes potential after n iterations.

* Upper limit of 15 iterations allowed. Almost converged to 3 significant figures.

FIGURE 1. Sphere in Strong Magnetic Field.
Guiding-Centers Moving on Cylindrical Shells.

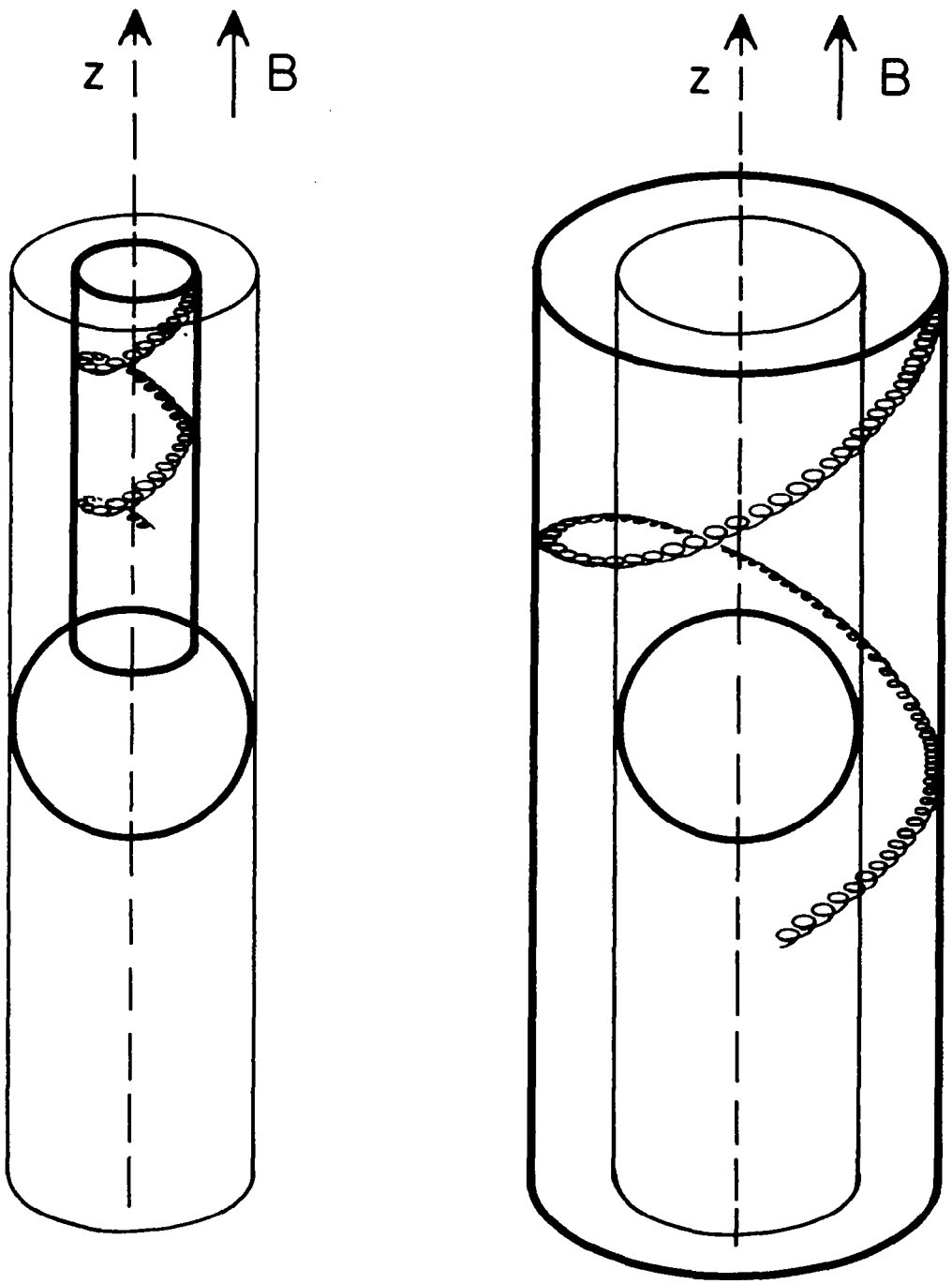

a. Shell which intersects sphere.

b. Shell which does not intersect sphere.

FIGURE 2. Drift Equation Solutions.
r vs z for various potentials.

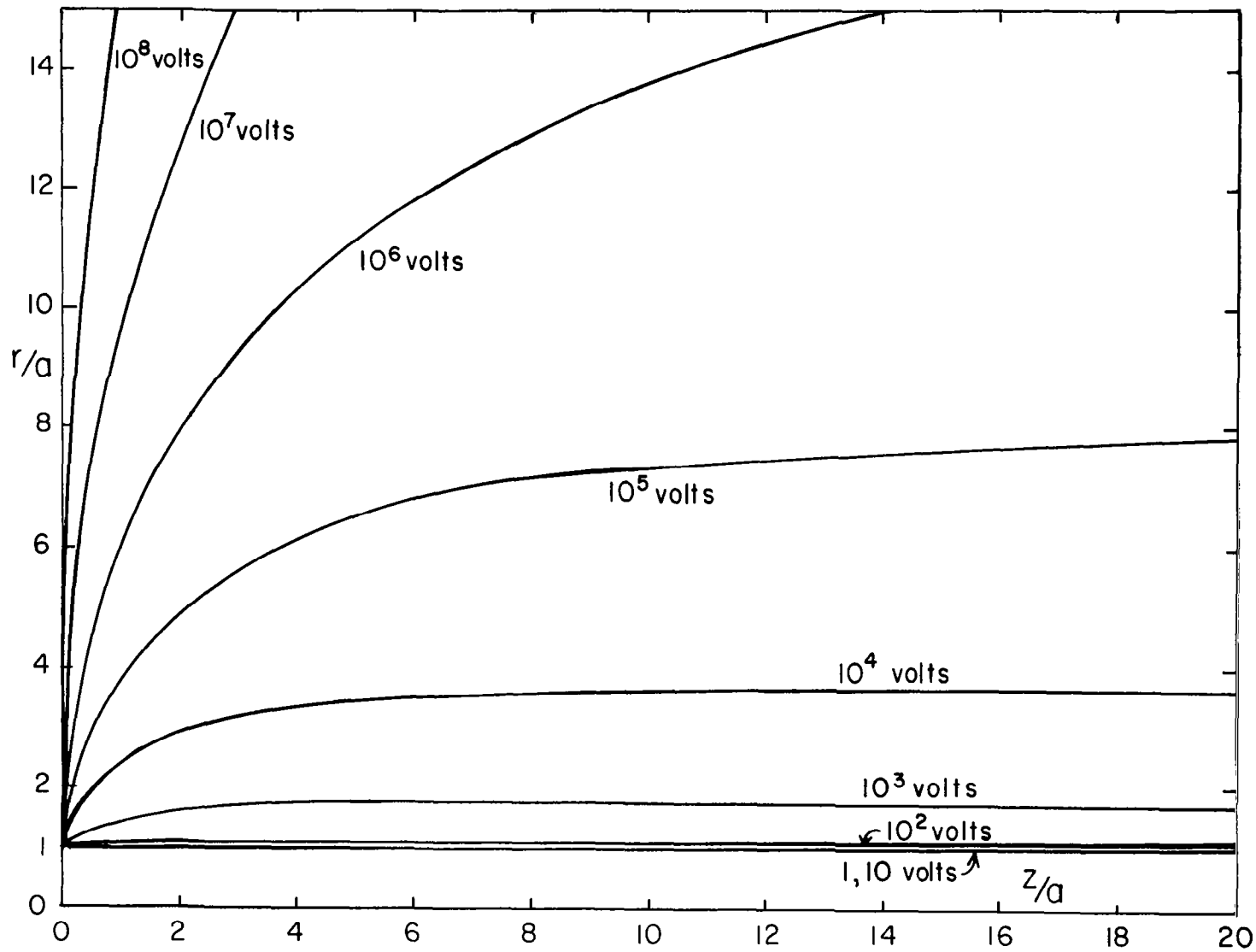

FIGURE 3. Limiting Radii vs Potential
from Drift Equation Solutions.

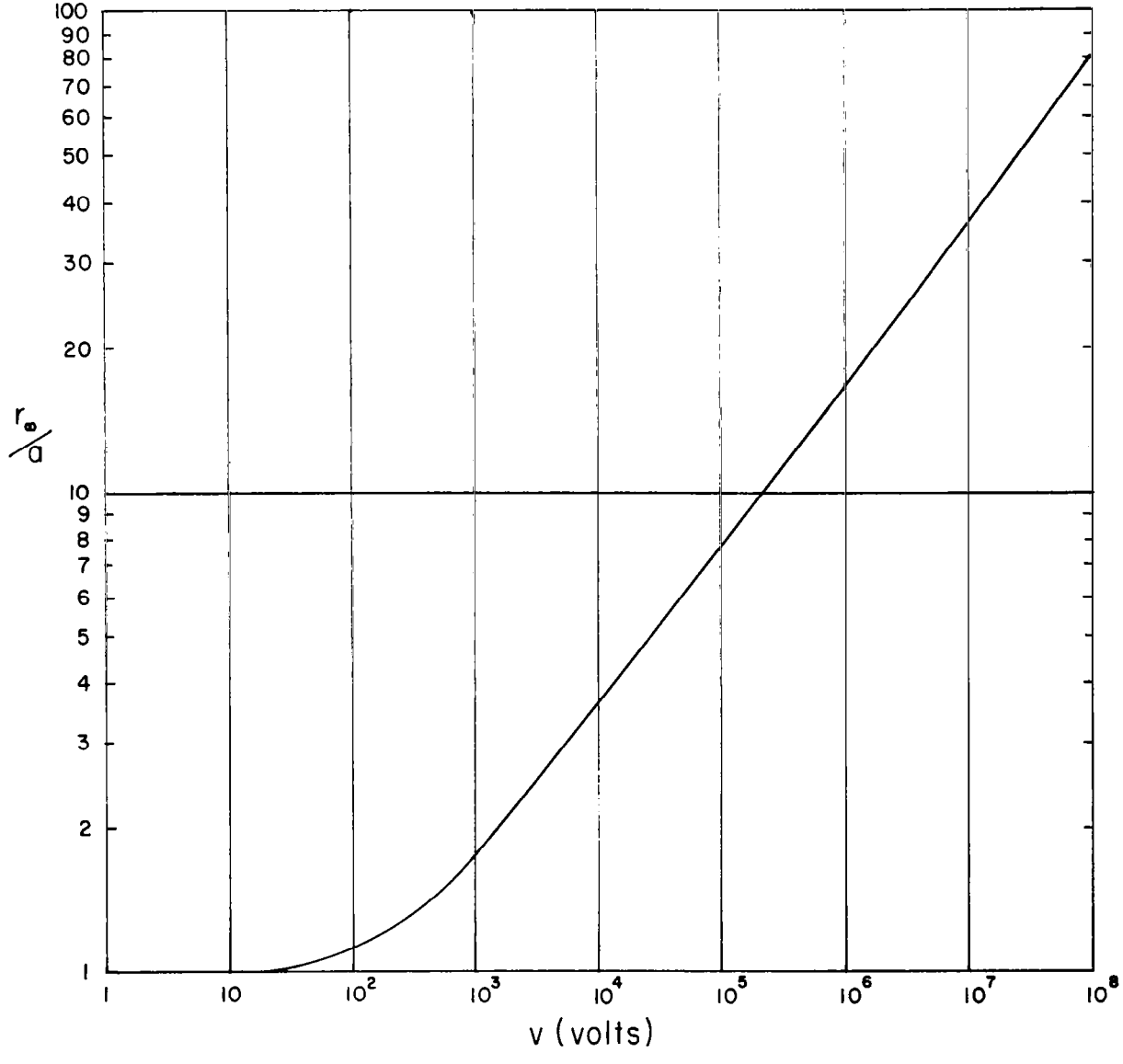

FIGURE 4. Magnetic Bottle - Initial Shell 2850 cm.

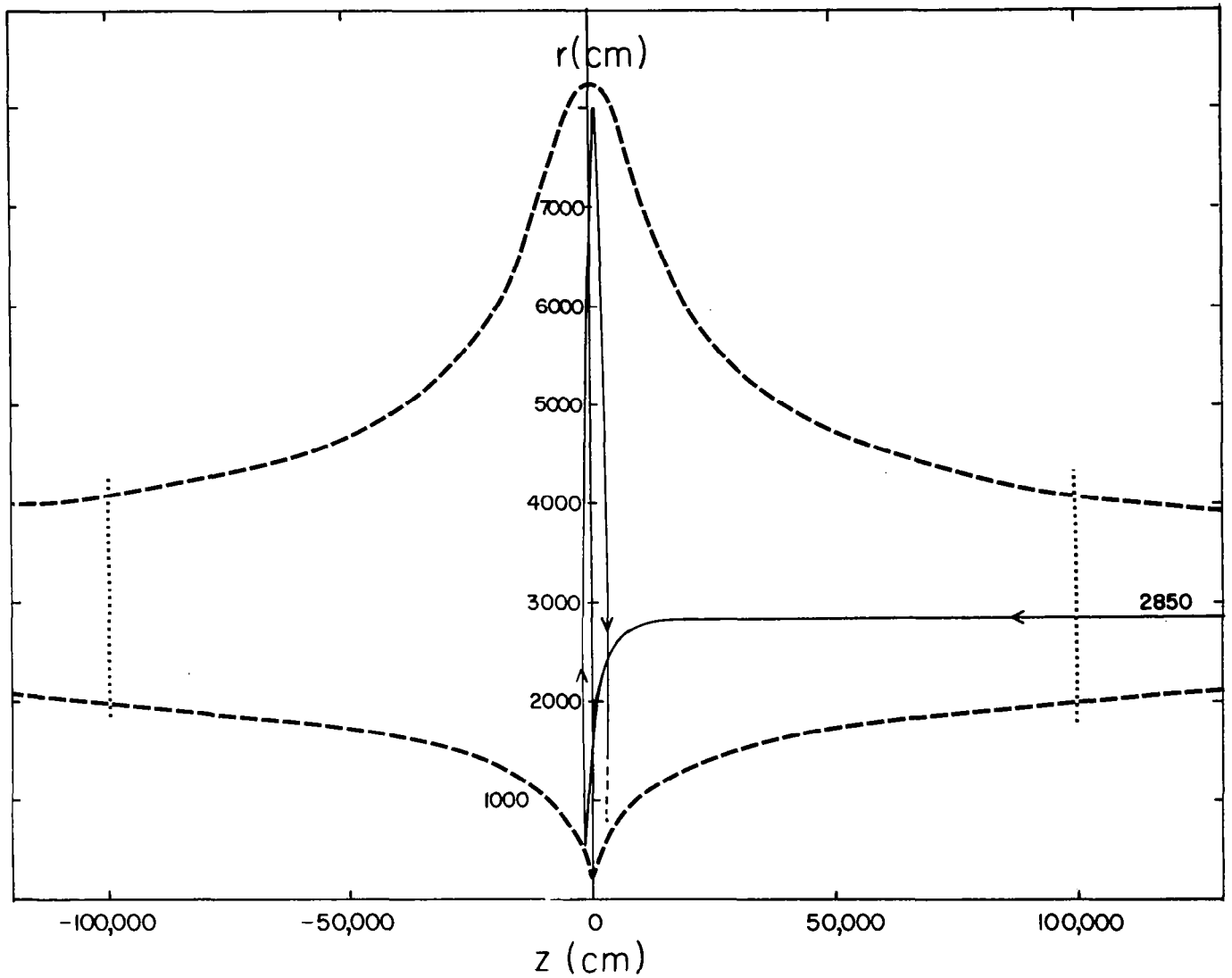

FIGURE 5. Vicinity of Sphere - Initial Shell 2850 cm.

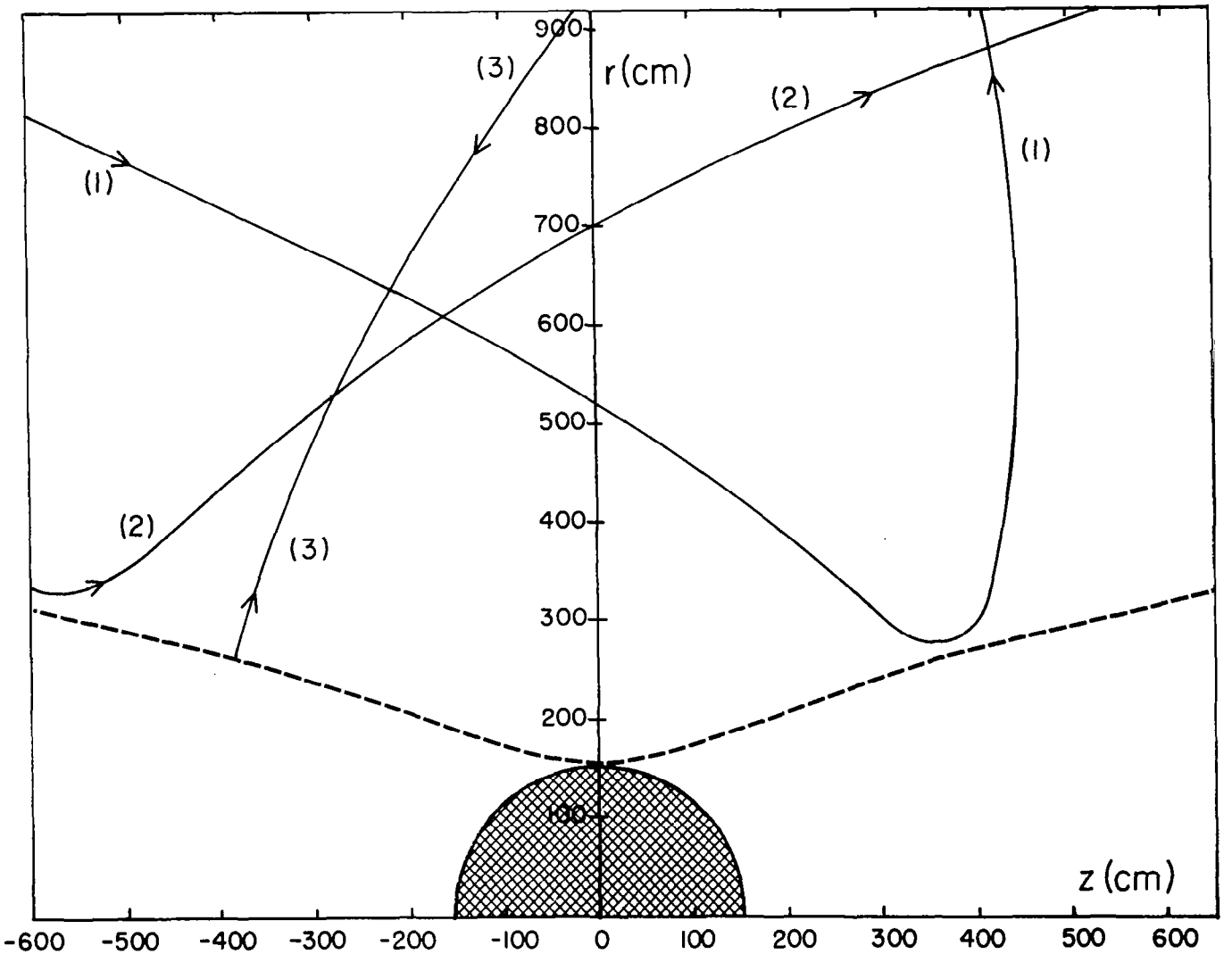

FIGURE 6. Magnetic Bottle - Initial Shell 1500 cm.

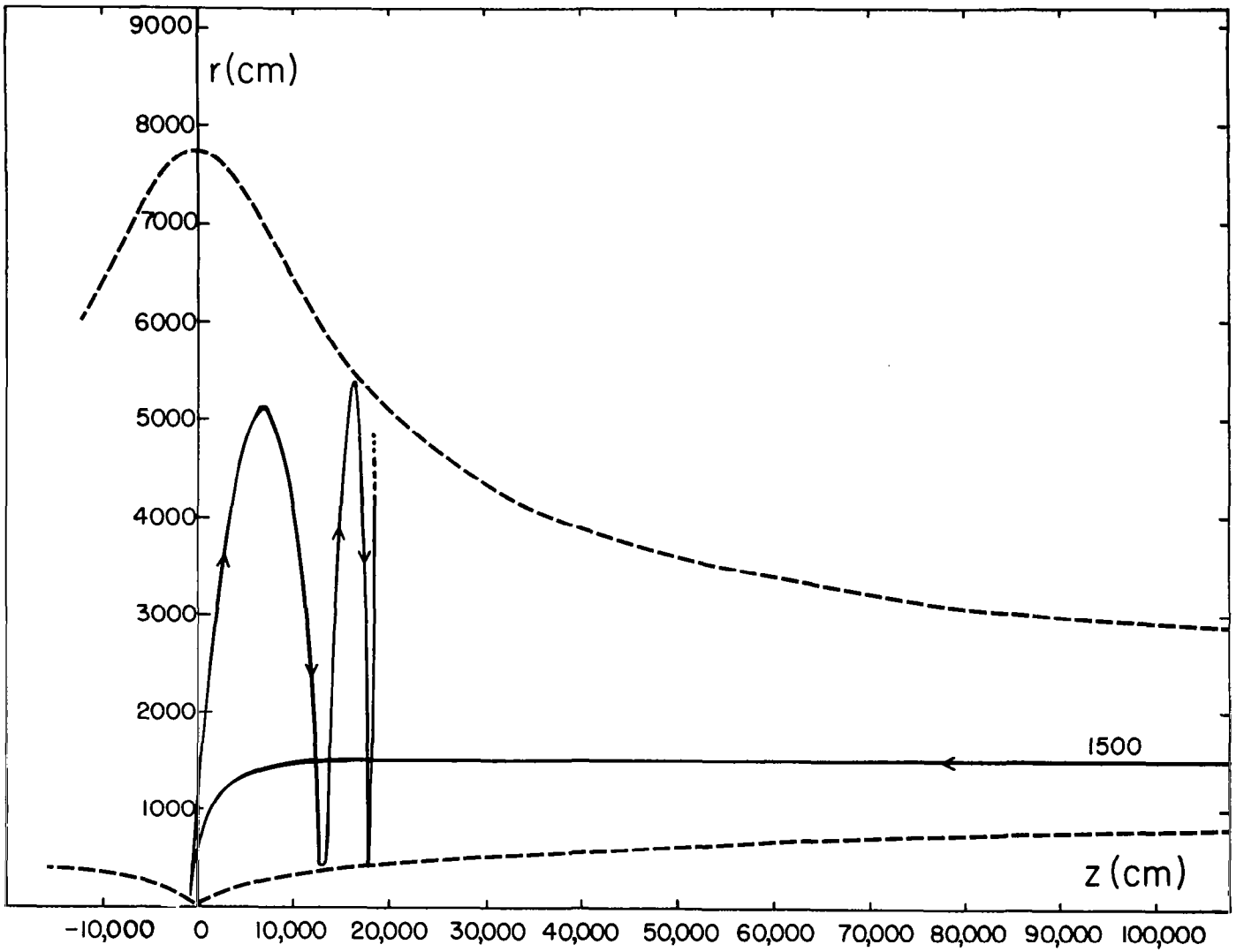

FIGURE 7. Vicinity of Sphere - Initial Shell 1500 cm.

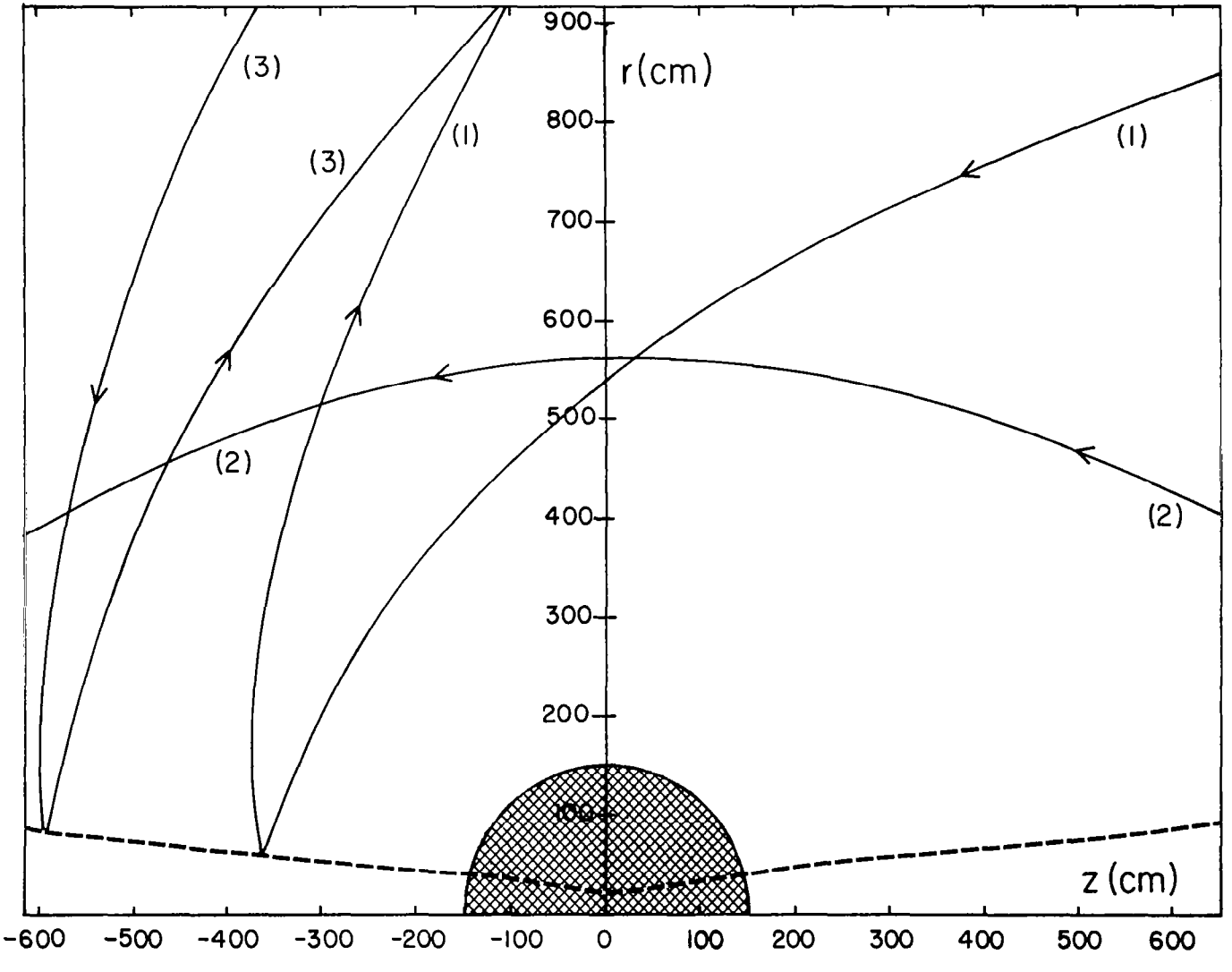

FIGURE 8. Magnetic Bottle - Initial Shell 1000 cm.

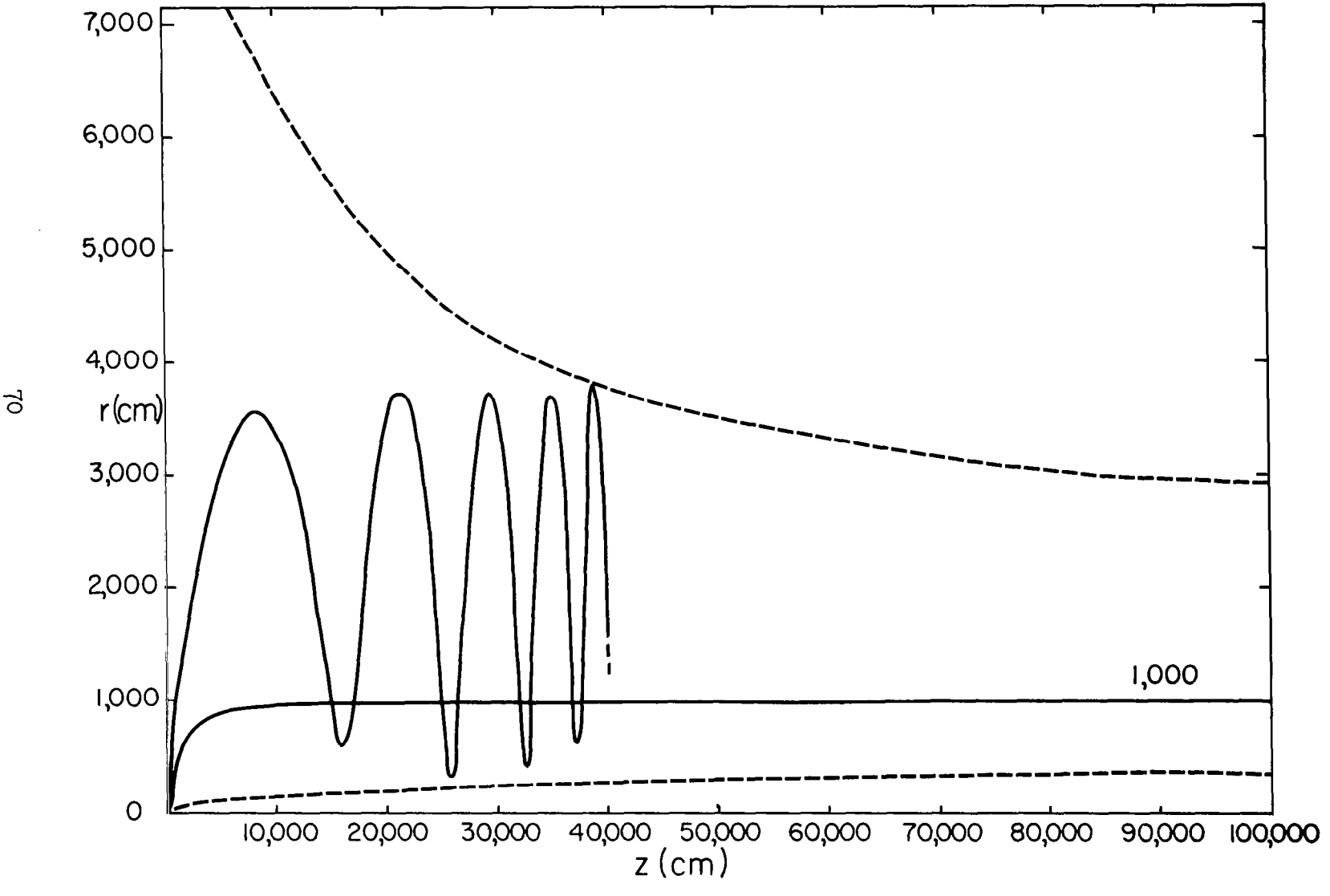

FIGURE 9. Vicinity of Sphere - Initial Shell 1000 cm.

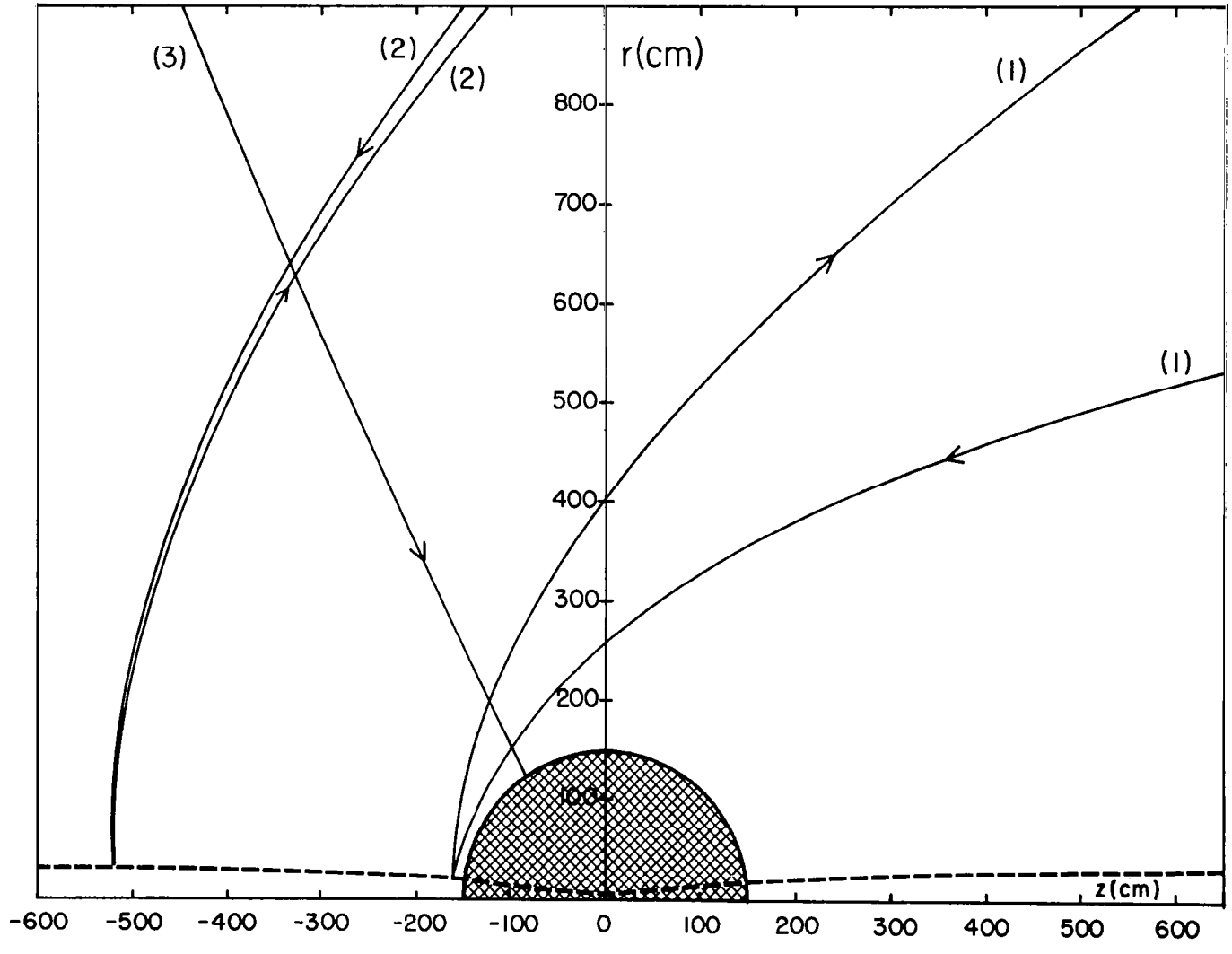

FIGURE 10. Grid in Spherical Coordinates for Poisson Calculation.

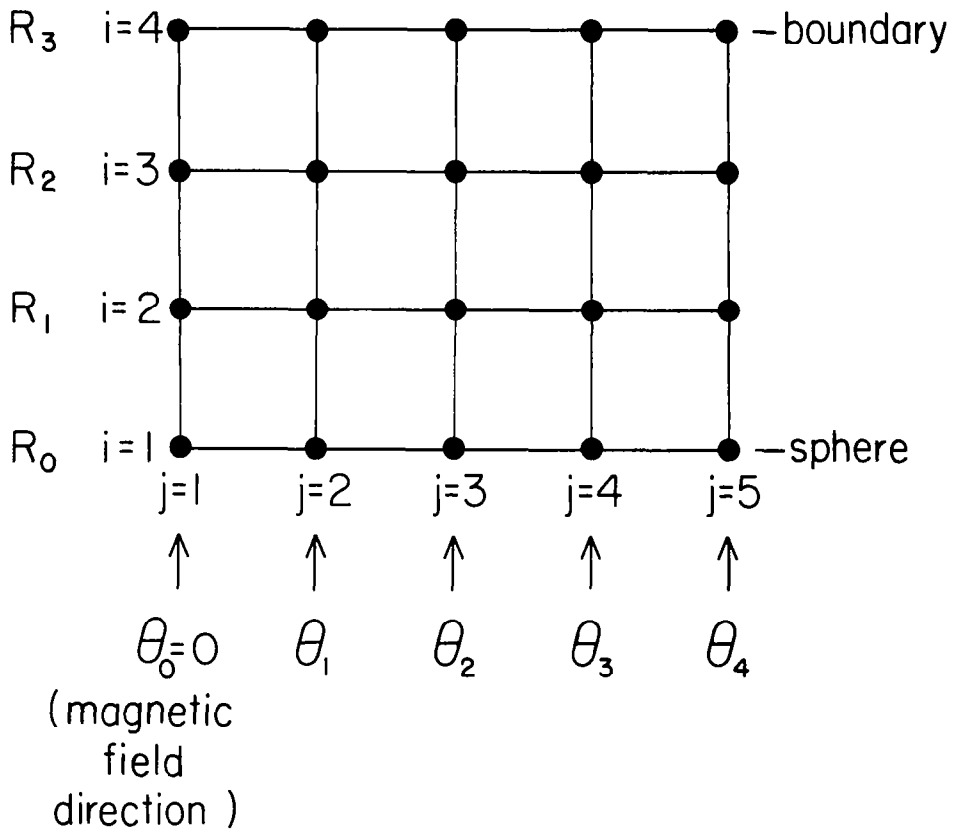

FIGURE 11. General Potential Distributions
for One-Dimensional Model.

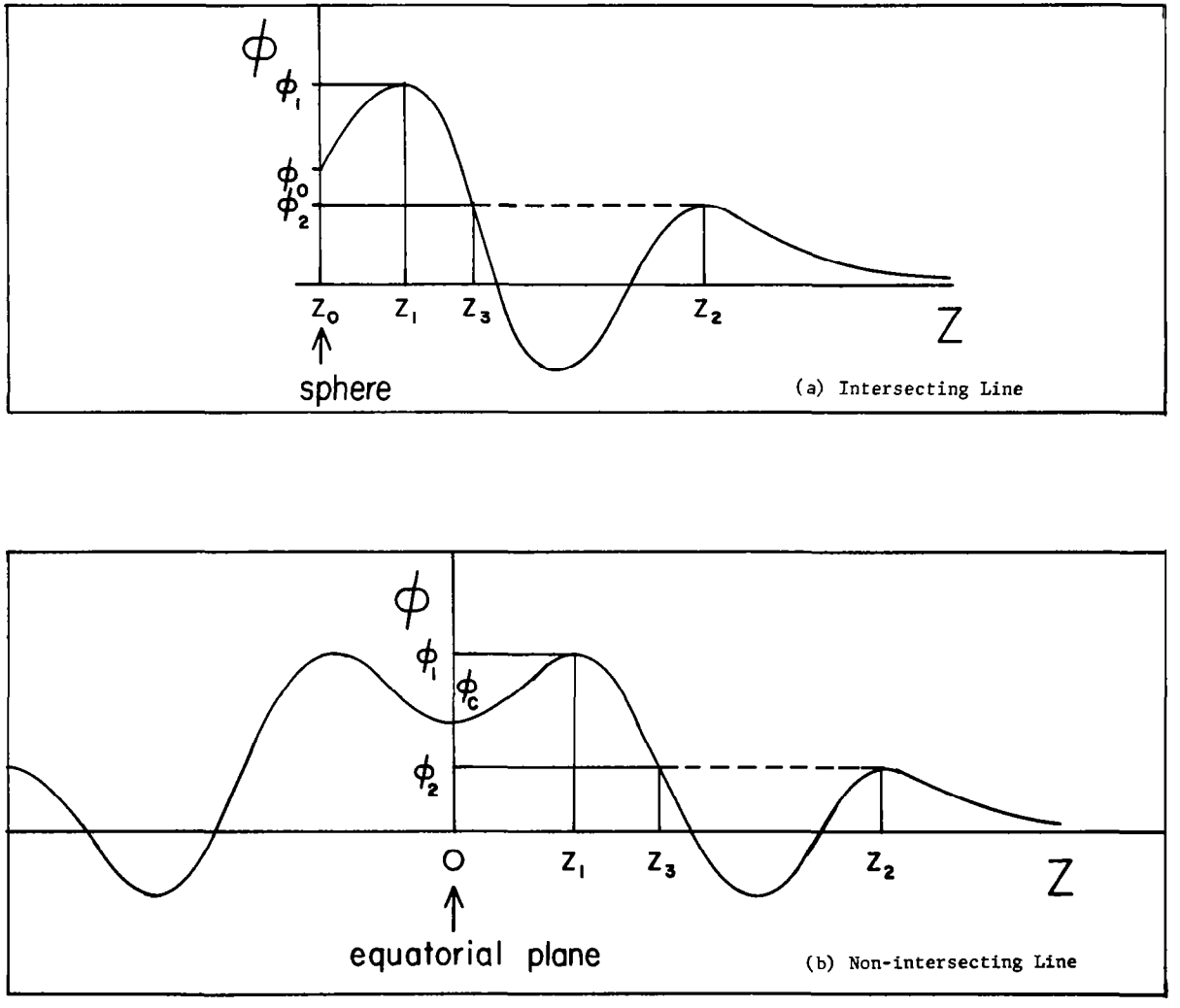

FIGURE 12. Simple Potential Distributions for One-Dimensional Model.

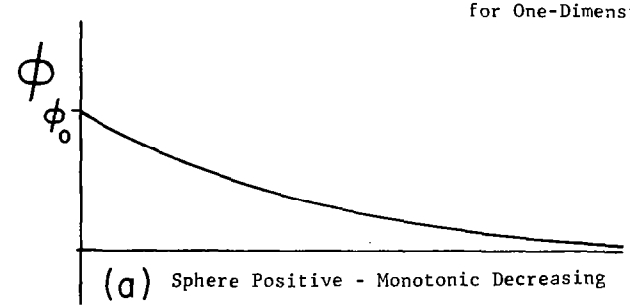

(a) Sphere Positive - Monotonic Decreasing

$$n = e^{-\phi}\left[1 - \tfrac{1}{2}\,\mathrm{erfc}\sqrt{\phi_0 - \phi}\,\right]$$

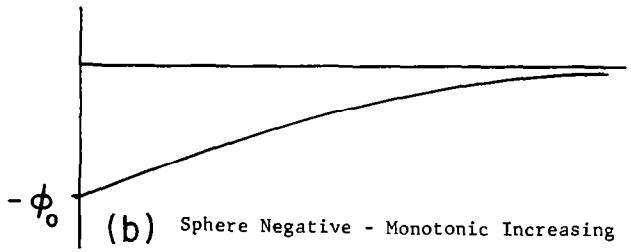

(b) Sphere Negative - Monotonic Increasing

$$n = \frac{e^{-\phi}}{2}\,\mathrm{erfc}\sqrt{-\phi}$$

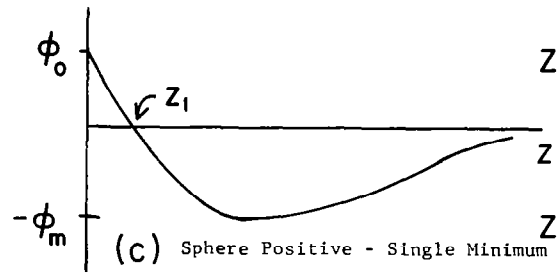

(c) Sphere Positive - Single Minimum

$$z < z_1: \quad n = e^{-\phi}\left[1 - \tfrac{1}{2}\,\mathrm{erfc}\sqrt{\phi_0 - \phi}\,\right]$$

$$z > z_1: \quad n = e^{-\phi}\left[\mathrm{erfc}\sqrt{-\phi} - \tfrac{1}{2}\,\mathrm{erfc}\sqrt{\phi_0 - \phi}\,\right]$$

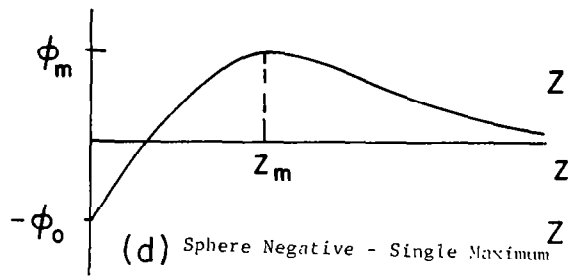

(d) Sphere Negative - Single Maximum

$$z < z_m: \quad n = \frac{e^{-\phi}}{2}\,\mathrm{erfc}\sqrt{\phi_m - \phi}$$

$$z > z_m: \quad n = e^{-\phi}\left[1 - \tfrac{1}{2}\,\mathrm{erfc}\sqrt{\phi_m - \phi}\,\right]$$

REFERENCES

1. D. Bohm, E. H. S. Burhop, and H. S. W. Massey, "The use of probes for plasma exploration in strong magnetic fields," in The Characteristics of Electrical Discharges in Magnetic Fields, ed. by A. Guthrie and R. K. Wakerling, McGraw-Hill, 1949. Ch. 2, Sec. 5.

2. B. Bertotti, "Theory of an electrostatic probe in a strong magnetic field," Phys. Fluids 4, 1047-52 (1961).

3. T. G. Northrop, The Adiabatic Motion of Charged Particles, Interscience, 1963. Ch. 1.

4. D. B. Beard and F. S. Johnson, "Ionospheric limitations on attainable satellite potential," J. Geophys. Research 66, 4113-22 (1961).

5. See, for example, H. M. Mott-Smith and I. Langmuir, "The theory of collectors in gaseous discharges," Phys. Rev. 28, 727-63 (1926).

6. I. B. Bernstein and I. N. Rabinowitz, "Theory of electrostatic probes in a low-density plasma," Phys. Fluids 2, 112-21 (1959).

7. J. Laframboise, "Theory of electrostatic probes in collisionless plasmas at rest," Fourth International Symposium on Rarefied Gas Dynamics, Toronto, July 14-17, 1964.

8. L. S. Hall, "The computation of self-consistent potential distributions in a collisionless plasma," University of California Lawrence Radiation Laboratory Report UCRL-7660-T, January, 1964.

9. L. S. Hall and R. P. Freis, "Theory of the electrostatic probe and its improved use as a diagnostic tool," University of California Lawrence Radiation Laboratory Report UCRL-12480, July, 1965.

10. Yu. M. Kagan and V. I. Perel', "Probe methods in plasma research," Soviet Physics Uspekhi May-June 1964 (Russian Vol. 81, Nos. 3-4) pp. 767-93.

11. A. H. Davis and I. Harris, "Interaction of a charged satellite with the ionosphere," in Proceedings of the Second International Symposium on Rarefied Gas Dynamics, ed. by L. Talbot, Academic Press, 1961.

12. F. Hohl and G. P. Wood, "The electrostatic and electromagnetic drag forces on a spherical satellite in a rarefied partially ionized atmosphere," in Proceedings of the Third International Symposium on Rarefied Gas Dynamics, ed. by J. A. Laurmann, Academic Press, 1963.

13. L. W. Parker, "A computer program for calculating the charge distribution about a space vehicle," National Aeronautics and Space Administration Contractor Report NASA CR-401, March, 1966.

14. L. W. Parker, "Theory of electrostatic planar and spherical probes," Mt. Auburn Research Associates Technical Report No. 3-16-66 (LWP-TR), NASA Contract No. NAS5-9088, March, 1966.

15. D. Greenspan, Introductory Numerical Analysis of Elliptic Boundary Value Problems, Harper, 1965. Ch. 5.

16. A. Ralston and H. S. Wilf, Mathematical Methods for Digital Computers, Wiley, 1960.